2011

Decision Aid Models for Resource Sharing Strategies During Global Influenza Pandemics

Alfredo Santana Reynoso
University of South Florida, alfredo_santana@hotmail.com

Decision Aid Models for Resource Sharing Strategies During Global Influenza Pandemics

by

Alfredo Santana Reynoso

A dissertation submitted in partial fulfillment
of the requirements for the degree of
Doctor of Philosophy
Department of Industrial and Management Systems Engineering
College of Engineering
University of South Florida

Major Professor: Alex Savachkin, Ph.D.
Tapas K. Das, Ph.D.
José Zayas-Castro, Ph.D.
Vernon Rego, Ph.D.
Yiliang Zhu, Ph.D.

Date of Approval:
June 8, 2011

Keywords: pandemic influenza, computer simulation, decision analysis,
resource management, international collaboration

Dedication

To my family, for their unconditional love and support.

Acknowledgements

I would like to thank my advisor Dr. Alex Savachkin for introducing me to the fascinating world of disease spread computer simulation. For his support and trust during this process. I am very grateful to all the other students of our group; they helped me with their work and inspired me with their example. I would like to give thanks to Andrés Uribe for working so hard on the simulation code that was the base of the one I used for this work; to Diana Prieto for her amazing job in reviewing the specialized literature and for bringing me on board for the USF Graduate School Challenge Grant that was the base of my work in Pandemic Influenza Surveillance Capacity Management; to Sharad Malavade for working with us in the Challenge Grant and sharing his medical expertise; to Dayna Martinez for her work on Non-Pharmaceutical Interventions; to Marbelly Davila for her guidance in the statistical analysis of the results using SAS, and to Sandro Paz for his work on U.S. Health Policy. I would also like to thank Meagan Eastman for her help editing this document.

I would also like to thank Dr. Lillian Stark for opening her lab to us and discussing at length the struggles they faced during the H1N1/2009 Pandemic. Special mention to Dr. Tapas Das for his help in the experimental design of our simulation and his insight in the 'big picture' of the project. My most deep admiration to Dr. Jose Zayas-Castro for pushing each student in the department to the border of our skills, and for constantly reminding us of the importance of stressing the intellectual merit and the broader impact of our work. To Dr. Yiliang Zhu for sharing with us his knowledge of Public Health and Biostatistics, and to Dr. Vernon Rego from the Distributed Computing Lab at Purdue University for his technical advice and for being patient enough to participate in all our meetings via the Internet.

Table of Contents

List of Tables

List of Figures

Abstract

Pandemic influenza outbreaks have historically entailed significant societal and economic disruptions. Today, our quality of life is threatened by our inadequate preparedness for the imminent pandemic. The key challenges we are facing stem from a significant uncertainty in virus epidemiology, limited response resources, inadequate international collaboration, and the lack of appropriate science-based decision support tools. The existing literature falls short of comprehensive models for global pandemic spread and mitigation which incorporate the heterogeneity of the world regions and realistic travel networks. In addition, there exist virtually no studies which quantify the impact of resource sharing strategies among multiple countries. This dissertation presents three related models that contribute to filling the existing vacuum. The first model develops optimal capacity management strategies for multi-region pandemic surveillance. The second model estimates the pandemic propagation time from the onset to a likely pandemic export region, such as a major transportation hub. The model builds on a large-scale agent-based simulation and geographic information systems (GIS). The model is tested on a hypothetical outbreak in Mexico involving 155 regions and over 100 million people. The third model develops an empirical relationship to quantify the impact of various U.S. - Mexico antiviral sharing strategies under several pandemic detection and response scenarios.

1. Introduction

Influenza is a respiratory infection caused by a virus which is endemic to the humans. However, sometimes a virus can attack more people than expected causing epidemics. Such epidemics can be identified by comparing the number of influenza like illness (ILI) cases to historical values. When an epidemic spreads to more than one country, or if the fatality or transmission ratios are very high, the epidemic is called a pandemic. The virus most often associated with pandemic influenza (PI) is that of type A. Influenza viruses are described by two key elements: hemagglutinin (H) and neuraminidase (N) (e.g., H1N1, H3N2, H5N1). Additionally, every year *antigenic shifts* can occur generating new virus subtypes. To cope with these changes, vaccines should be formulated periodically [2]. When a novel virus subtype adapts to the human population, our bodies can no longer develop immunity. Consequently, a PI outbreak can start. The duration of an outbreak, the number of people and regions affected, and the mortality ratio are directly related not only to how the virus is transmitted, but also to the social and demographic characteristics of a society.

On May 9 of 1997, the first human case of H5N1, also known as Avian Flu, appeared in Hong Kong [3]. A major slaughter of chickens was implemented in an attempt to stop the bird-to-human transmission [4]. Nowadays, the World Health Organization (WHO) has declared H5N1 human outbreaks in fifteen Asian and African countries with a total of 438 infected cases, and the 59.8% case fatality ratio [5].

On March 18 of 2009, the Mexican government reported a suspicious ILI outbreak in rural areas in the south of the country. By April 4, WHO confirmed that the infection cases were caused by an aggressive novel subtype of influenza virus A/H1N1 [6]. At the end of April, WHO reported that this new subtype of H1N1 had been

confirmed in several countries with over 182,166 cases. In the American continent, approximately 1,579 of the 1,799 deaths were reported [7]. By mid-October, WHO reported 400,000 confirmed cases, with at least 4,735 deaths, worldwide [8].

Despite the facts that the H5N1 virus is believed to be transmittable only by eating food contaminated with fresh bird feces and that human-to-human transmission has not been confirmed yet, there exists a major concern due to potential mutations of the virus which can combine its code with another influenza virus capable of a human-to-human transmission.

Nowadays, the international community has both antiviral drugs to reduce the impact of influenza, and a capability to produce vaccines in a few months once the virus is isolated and identified. However, antiviral drugs are perishable items that cannot be stored in large quantities for long periods of time due to cost constraints. On the other hand, at present vaccines are produced using a 50-year technology, making it difficult to accurately forecast the production output. Additionally, a high level of population compliance to vaccination campaigns is needed to stop the spread of a pandemic. Past unfortunate experiences can affect the risk attitudes of the population during vaccination campaigns. For example, a major public health vaccination campaign was conducted by the United States government in 1976, trying to prevent a major pandemic of H1N1 that did not actually happen. Major lawsuits and allegedly vaccination-caused diseases established legal and social precedents which need to be considered by public health officials today [9].

Figure 1 shows the world population density (from white to red) and the world airports (green dots). It can be seen that most of the airports are concentrated in the U.S. and Europe. Consequently, once an outbreak reaches these regions, it will be almost impossible to contain the spread and hence a global outbreak will be inevitable. On the other hand, it has been discussed in the literature [10] that it is probable that an outbreak would start in a high density region in a poor rural area (most of them

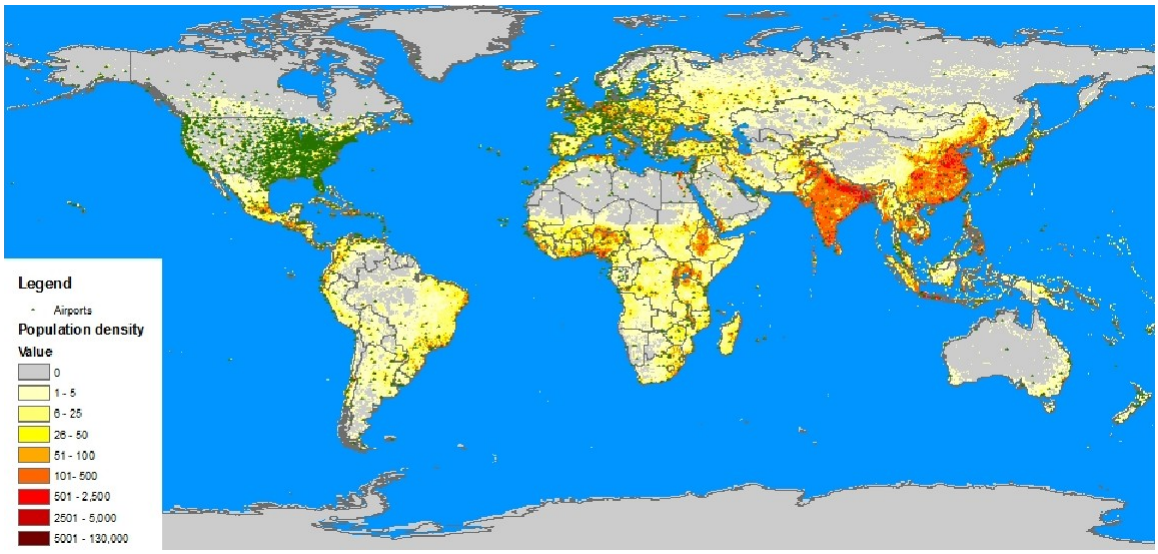

Figure 1: Map of the World Population Density and Major Airports

represented in red in Figure 1). However, with the exception of Southeast Asia, most of these areas lack an effective PI surveillance system. As a consequence, when an outbreak starts in one of these regions, it is just a matter of time before infected travelers reach a region with a major travel hub. From that moment, it is just a matter of days for the outbreak to spread around the world. This effect was observed during the H1N1/2009 PI outbreak.

The possible global economic impact of PI was analyzed in a study developed by the Lowy Institute for International Policy coordinated by experts of the Australian National University [11]. This study analyzed four scenarios of PI: mild (H3N2 1967-68 equivalent scenario), moderate (H2N2 1957-58 scenario), severe (1918 Spanish flu scenario), and an ultra severe scenario (1918 Spanish flu scenario affecting equally every demographic group in the population). By analyzing these scenarios, the authors estimated that in our time a PI outbreak would cost a country between 1.5% and 5% of its gross domestic product. This impact is attributable to school and company closures, (in)voluntary workforce reduction, and medical expenses. In the case of the United States, the estimated impact ranges between $73.1 to $166.5 billion dollars. The same study estimated the number of deaths in the U.S. to be 20,000

(mild scenario), 200,000 (moderate scenario), 1M (severe scenario), and 2M (ultra severe scenario).

Inefficiency of the global PI surveillance network can negatively affect the U.S. preparedness in the event of a global PI outbreak. Furthermore, the U.S. also faces some domestic preparedness and response issues. The first issue is related to the cost and accuracy of the tests for virus diagnosis. The higher costs of more accurate tests makes it economically infeasible to apply the tests to all individuals who present ILI symptoms. On the other hand, low reliability (false negatives up to 70%) of more economic and rapid tests can make medical personnel believe that even negative results may be positive [12]. The second issue is that there exists a constrained supply of response resources. For example, antiviral drugs are available for just a fraction of the total population (the U.S. stockpile was only 6.7% of the population in 2008 [13]). There can also be delays in the production of vaccines. Moreover, it is estimated that up to 65% of the U.S. population would not be willing or would decide not to receive the vaccine [14]. The existing pro-rata policy of the department of Health and Human Resources (HHR) establishes a distribution of mitigation resources in proportion to the population in each affected state [15]. However, this policy assumes that all affected states have homogeneous affected population and simultaneous outbreaks. As a result, extra resources can be assigned to regions where the outbreak is mild or where the peak has already passed, while limited resources will be left to regions where the outbreak is just beginning. Finally, the U.S. lacks a clear international collaboration policy in the case of overseas-born PI outbreaks.

There exists a strong motivation for the U.S. to explore international collaboration. If an outbreak starts overseas and is detected promptly, and if the country of origin has appropriate pharmaceutical and non-pharmaceutical interventions in place, then the outbreak may be contained at the source [16]. However, developing countries may not have enough supply of antiviral drugs, or their detection capabilities and health

care infrastructure may be limited. Additionally, the countries may lack required expertise to efficiently implement non-pharmaceutical interventions [17]. By sharing pharmaceutical repositories, giving financial aid to develop proper surveillance and health care systems, and training public health officials, the U.S. may help to protect its population domestically. There is also a benefit that developing countries can share their virus strains in a timely manner, so that the samples can be included in the design of a vaccine [17]. Hence, the important question is how much and what resources to share to delay, and possibly avoid, the arrival of overseas-born pandemics to the U.S. soil.

Our research contributes to the development and improvement of the U.S. mitigation strategies during global influenza pandemics. In Chapter 2, we analyze the status of the relevant academic literature and identify most significant gaps. Chapter 3 describes our research objectives. Chapter 4 presents a model to develop optimal capacity management strategies for PI surveillance. Chapter 5 presents the agent-based simulation model to estimate the outbreak lead time from the onset to a likely pandemic export region for the testbed of Mexico. Chapter 6 develops an empirical relationship for the outbreak lead time in order to examine U.S. - Mexico antiviral sharing strategies in global pandemic scenarios. Chapter 7 summarizes the main results, contributions, and future research opportunities.

2. Literature Review

We classify the existing PI models into three main categories: statistical, dynamic compartmental, and simulation-based models.

The main objective of the *statistical models* is to estimate epidemiological parameters with the use of statistical analysis and/or optimization tools, such as maximum likelihood estimation, Markovian analysis, linear programming or regression-based approaches. For example, Carrat et al. applied Markovian models to compare the short-term influenza immunity obtained from vaccination to the long-term immunity acquired from actual infection. The authors demonstrated that yearly vaccinations during young years could make an individual more prone to the disease in his senior years [18]. Becker and Starczak evaluated the effectiveness of a vaccination campaign using a linear programming model. Considering constraints on resource availability, the model aimed to optimize the expected reproduction number by selecting the proportion of people in each household to be vaccinated [19]. In their classic 1982 paper, Longini and Koopman applied the maximum likelihood principle to fit a statistical model to symptom related data [20]. More recently, Yang, Longini and Halloran applied the same methodology to estimate the transmission probabilities and the efficacy of prophylactic interventions [21]. The authors took data from two trials in 2001 and 2004 using the antiviral drug osteltamivir (also known as Tamiflu). The paper estimated a reduction in the probability of infection by 85% for exposed cases, and a reduction in the probability of transmission of 66% for infectious individuals [21]. Cauchemez et al. used Markov chain Monte Carlo sampling to model the risk of household-based and community-based infection. The paper concluded that children were more prone to influenza than adults in 79% of cases, and that they had higher

risk from community born infection in 76% of cases [22]. In the example papers above, some models used simulation as a validation mechanism or a tool for deriving numerical conclusions.

Dynamic compartmental models have mostly focused on describing the natural history of influenza. Typically, each individual in the population is assigned to a compartment. However, this model does not address some important aspects of the disease such as the latency period, or the fact that some infected individuals never develop symptoms. To model the transitions among compartments, most models use tools such as Markov chains and differential equations. It is widely accepted that the Markovian assumption of dependency only on the previous stage is reasonably valid for modeling influenza like diseases.

Ball and Lyne explored different vaccination policies using three dynamic compartmental models: Susceptible, Infected, Recovered (SIR), Susceptible, Infected, Susceptible (SIS), and Susceptible, Infected, Recovered, Susceptible (SIRS). The three models represented permanent, non-existent, and temporary immunity, respectively, after the individual was infected [23]. Most of the dynamic compartmental models assume homogeneity of the population. Larson attempted to build more heterogeneous populations by developing three models that divided the population in the groups of active/inactive, working/non-working, and changing social distancing and personal hygienic behavior [24]. While the models increased in their complexity, the conclusions were still very aggregate.

Arino et al. stated that complex compartmental models can yield similar conclusions as simulation-based models. The authors used nine states of which two were Susceptible-Latent-(A)Symptomatic-Recovered models, with and without treatment, respectively. The recovered state was shared, and latent and infected individuals could obtain or decline medical treatment [25]. The models assumed homogenous population in each compartment, and did not include any type of non-pharmaceutical inter-

vention or consideration of social dynamics. Consequently, the model only emulated the conclusions of agent-based simulation models in the estimation of pharmaceutical interventions using antiviral drugs. Atkinson and Wein designed a more complicated variation of these models in an attempt to quantify the routes of influenza transmission. Based on previous medical studies, they concluded that aerosol based transmission (e.g., by sneezing) is the dominant mode of transmitting influenza. However, the authors also acknowledged that their conclusions were not definitive and other types of transmission (e.g., through contaminated surfaces) could not be discarded [26].

Mathews et al. argued through historical evidence that after recovering, an individual can present long-term or short-term immunity. They built a model that, besides the latent-(non-)infectious and (a)symptomatic stages, included these two new stages. The authors fitted their model with records from 1918 and 1971 PI from some remote British territories. They concluded that for individuals that had been isolated from endemic influenza, PI could be more aggressive due to the lack of heterosubtypic immunity created by individuals living in societies with endemic influenza [27]. As it can be concluded from the above examples, some important observations can be drawn regarding the natural history of influenza using dynamic compartmental models. However, the complexity of PI outbreaks in a heterogeneous and dynamic society can not be adequately analyzed by using these types of models.

Because of the complexity of the issues surrounding PI outbreaks, it is highly challenging to build a purely mathematical model of a heterogeneous population with diverse social interactions. *Simulation models* have been used to address these challenges. Another benefit of simulation models is an explicit consideration of randomness of events. This is done by using random variables. By running a model several times and modifying the values of some key parameters, sensitivity analysis can be performed to estimate the confidence intervals for the output variables. Below we provide a sample of representative simulation-based models.

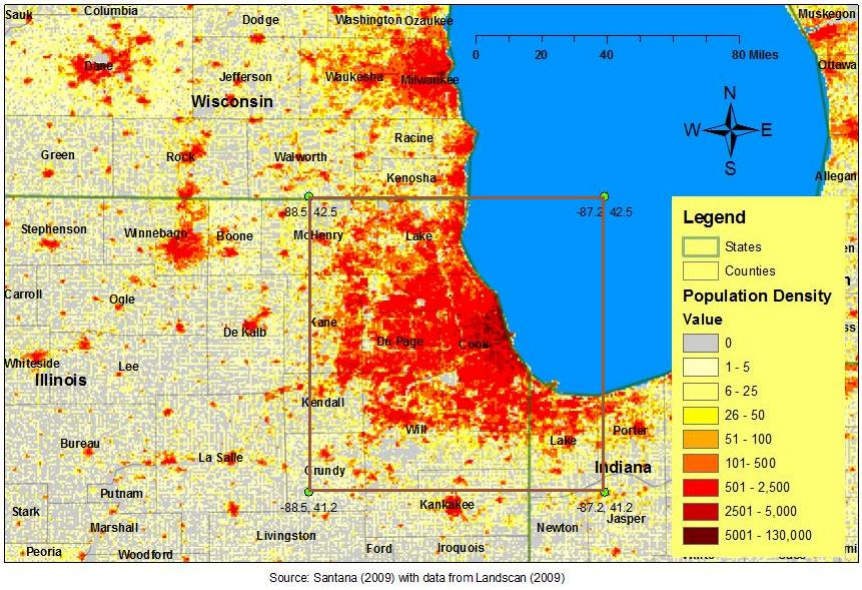

Source: Santana (2009) with data from Landscan (2009)

Figure 2: Chicago Defined as a Metropolitan Area by Halloran et al [1]

A collaborative network of researchers supported by the National Institute of General Medical Sciences and the National Institutes of Health (NIH) created the Models of Infectious Disease Agent Study (MIDAS). Despite the fact MIDAS was not created exclusively to study PI, three major models [28–30] were developed to study a set of interventions known as targeted layered containment (TLC). The objective of TLC is to study the synergetic effects of various interventions, such as targeted use of antiviral drugs, isolation of infected individuals, quarantine of affected households, school and workplaces closure, and social distancing. Halloran et al. developed a cross validation of the MIDAS models using the data of 8.6 million people in the city of Chicago [1]. For this purpose, the authors partitioned the Chicago Metropolitan Area by using geographic coordinates, as shown in Figure 2. By doing that, the authors were able to identify metropolitan regions in a specific geographic context. However, it can be observed from the map that using square-shaped boundaries may not be the best approach to define a region.

Ferguson et al. used geographic information systems (GIS) to incorporate demographic densities obtained from LandScan [31] into an epidemiological model. The

model incorporated a heterogeneous population of households and three types of schools and workplaces, distributed randomly according to the population density. The authors modeled Thailand [10] and the continental U.S. and U.K. [28]. The assumptions regarding transmission of PI in schools were conservative compared to similar models. As a result, the conclusions did not emphasize school closures. Ferguson et al. developed a force of infection transmission model based on the probability of getting infected according to the theoretical basic reproduction number (R_0). The authors also presented a comprehensive air travel network for their U.S.-U.K. paper. However, it was assumed that infected people arrived to the main airports of the countries at a fixed rate. This assumption made it difficult to assess the conclusions regarding global outbreaks outside the regions of study.

A typical small U.S. town was modeled by Glass et al. The contact process was based on the Ferguson et al. model[28], but the authors used fixed and random links to relate a network of 10,000 individuals and neighborhood contacts. More emphasis was given to the contact among children and teenagers in two types of schools. As a result, school closure proved to be the most reliable type of intervention [32]. Another MIDAS model was created by Germann et al., based on the transmission process considered by Longini et al. [16]. The model considered 281 million people residing in the continental U.S. and R_0 from 1.6 to 2.4. The paper concluded that it was important to apply travel restrictions in addition to other interventions which can help to reduce the spread of the outbreak and gain additional time. However, travel restrictions by themselves seemed to be not very effective [29].

Wu et al. modeled a single region (Hong Kong City), adding an infectious pre-symptomatic stage in the incubation period of the natural disease history. As a result, they concluded that household-based interventions were more important, even if the compliance level was relatively low. They also suggested an algorithm to implement isolation, quarantine, and antiviral prophylaxis in six different scenarios: no

interventions; quarantine; quarantine and isolation; quarantine and antiviral drugs; quarantine, isolation; and antiviral drugs, and quarantine, isolation, antiviral drugs with contact tracing [33]. Some of the strategies were economically unfeasible because they required up to 12 doses of antiviral drugs per individual in the population. As a reference, in 2006 the U.S. stockpile was only five million doses [29].

Historical data from a 2003-2004 influenza outbreak in six North Carolina counties were used by Cooley et al. to fit an agent-based simulation model with ILI records from local authorities. The model, which included schools, workplaces, public transportation, households, neighborhoods and communities, achieved a strong fit with historical data [34]. Los Alamos National Lab developed an epidemic simulation engine called EpiSimS, a discrete agent-based simulator, that was used to model Southern California with data from the 2000 Census. Mniszewski modeled six counties in California with a total population of almost 19 million individuals divided into six million households and almost a million locations, such as business, schools, shops, and restaurants. Some scenarios of the study, for example, closing school for up to six months, did not seem to be realistic [13].

Das, Savachkin and Zhu developed a large-scale simulation model for 1.1 million people distributed in 400,000 households. The model featured a high level of granularity, including hourly schedules for each individual and hour-by-hour interactions to simulate the contact process. The model included a total of thirteen different types of community establishments. Pharmaceutical and non-pharmaceutical interventions were simulated, and detailed statistics were collected including the cumulative numbers of infected and dead, the total cost of medical care, and lost productivity [35]. This model was one of the most detailed simulation found in our review of the academic literature, but also one of the most demanding in terms of computing resources.

Uribe et al. designed a multi-region testbed for Florida using detailed demographic and social information for the counties of Hillsborough, Dade, Leon and Duval [36].

The definition of a metropolitan area using only county data may be inadequate, because part of the metropolitan population that live outside the county may not be included (for example, Pinellas County in the case of Tampa or Broward County in the case of Miami). On the other hand, rural areas of the county may not be so relevant for simulation purposes. However, the conclusions of their work were not affected by this issue. The authors were able to demonstrate that the current pro-rata policy of pharmaceutical distributions of resources among counties was not optimal. The study designed a simulation-based optimization model to distribute such resources in a more efficient way, thus decreasing the total cost of the outbreak.

To the best of our knowledge, there has been only a few global PI simulators developed. The IBM Eclipse group built the Spatio-Temporal Epidemiological Modeler [37]. However, this model is based on a network of regions with completely homogeneous populations. PI propagated from one region to another only by ground transportation, in proportion to the length of the common boundaries between adjacent regions. Inside each region, simple dynamic compartmental models like SIR calculated the number of infected and recovered using differential equations.

Colizza et al. [38] took a different approach by using a global air travel network [42]. The model connected most of the world cities (2094) with international airports. However, the population within each city was homogeneous and the outbreak model followed the SEIR model. Moreover, there was no consideration of the rural area surrounding each one of the metropolitan areas. A different study showed that a selected sample of 155 airports including 100 most important cities produced similar results with less computational load [43]. Table 1 summarizes the above simulation models.

Academic papers focusing on international collaboration to reduce the impact of PI are mostly in the form of qualitative studies. A sample of these papers is shown in Table 2. There exist some studies discussing national and multi-national

Table 1: Simulation-Based PI Containment and Mitigation Models

Author, year	**Single region (SR) / Cross regional (CR)**	**Objective**	**Key features**
Ferguson et al, 2005 [10] and Ferguson et al, 2006 [28]	SR-2005(Thailand) and CR-2006 (US & UK)	Model PI spread & assess mitigation strategies	- Use of GIS (Landscan) - Targeted mass prophylactic use of antiviral drugs and social distancing - Heterogeneous among groups, homogeneous within group - 85M Thailand, 300M US, 58.1M UK
Glass et al, 2006 [32]	SR (small town in New Mexico)	Examine role of social distancing	- Targeted social distancing to mitigate PI - Fixed, small-scale contact network - Transmission rule follows exponential distribution - Emphasis in children and teenagers
Germann et al, 2006 [29]	SR (US)	Assess mitigation strategies	- Sensitivity analysis on R0 from 1.6 to 2.4 - Artificial 281M individuals from 2000 US census data divided in 2000-person communities - Long trips modeled after Bureau of Transportation data
Wu et al, 2006 [33]	SR (Hong Kong)	Test different intervention scenarios	- Natural history includes infectious presymptomatic - Suggest household-based interventions - Requires high stocks of anti-viral drugs
Colizza et al, 2007 [38, 39]	CR (global)	Model worldwide spread of a pandemic with air travel	- Air travel network - Urban centers - Compartmental models (SLIR) - Analysis of antiviral and travel restrictions
Halloran et al, 2008 [1]	SR (Chicago)	Cross-validate targeted layered containment models (Ferguson/Germann/Eubank)	- Chicago metropolitan area (8.6 million people) - R0 from 1.9 to 3.0 - Simulate effectiveness of feasible intervention strategies
Cooley et al, 2007 [34]	SR (NC)	Compare real life pandemic curve against simulation	- Use of 2003-2004 NC outbreak data - Use ILI data to estimate model parameters - Curve fitting exercise
Das, Savachkin and Zhu, 2008 [40]	SR	Mimic stochastic propagation of PI	- Large-scale model - Hourly schedules - Heterogeneous population (1.1 M)
Savachkin et al, 2009 [41]	CR (4 counties, Fl)	Model PI spread & assess mitigation strategies	- Dynamic predictive strategy test bed (4M people) - Optimization model for resource allocation - Minimize total cost of the outbreak
STEM-Eclipse,2009 [37]	CR (global)	Model PI spread	- Geographic visualization of PI spread - SIR model - Only ground travel

Table 2: Literature on International Collaboration

Author, year	**Objective**	**Key features**
Guimera, 2005 [42]	Design an optimal global airport travel network	- Used in subsequent papers by Colizza and others
Fraser, 2009 [54], Colizza, 2009 [61], and Lipsitch, 2009 [62]	Estimate the number of infected cases during H1N1 outbreak in Mexico	- Domestic air travel - Homogeneous population - SEIR models - Results varied from 2K to 1.4M
Patel, 2008 [44], Hanvoravong, 2010 [45], Mensua, 2009 [46], and SPPNA, 2007 [47]	Compare national PI preparedness plans (qualitative discussions)	- UK, US, NZ, CAN, AUS - SE Asia - Latin America - North America
Franco, 2009 [51], Gallaher, 2009 [52], and Katz, 2009 [53]	Conduct qualitative analyses of H1N1 2009 outbreak; recommendations for preparedness	- Accurate outbreak chronology - Comparison to 1918 outbreak - Revise international regulations
McDougall, 2008 [48], Oshitani, 2008 [17], and Paranthaman, 2008 [49]	Suggest international collaboration	- Qualitative discussions
Thompson, 2006 [50]	Analyze ethical aspects in pandemic preparedness	- Qualitative discussion

PI preparedness plans [44–47]. Another set of papers presented arguments in favor of international collaboration [17, 48, 49]. However, the discussion was centered on ideas which were not supported by quantitative data. The ethical aspects to consider in pandemic preparedness were also argued in the literature [50]. In the last two years, a significant number of papers were published regarding the H1N1/2009 experience [51–60]. Some of these papers included quantitative analysis, either using data collected from the outbreak or from simulation models trying to emulate its behavior. However, the discussion on international collaboration in these papers was limited.

In October of 2006, a committee from the Institute of Medicine (IOM) put a set of recommendations to enhance the existing pandemic models. The most relevant recommendations for our research are the following: (i) to develop improved estimates of model and parameter uncertainty, (ii) to include a broader range of closure options, (iii) to include costs and benefits of intervention strategies, (iv) to design models that

will help policy makers establish strategies and policies, (v) to include decision-aid models that can be linked to surveillance data to provide real-time feedback, (vi) to consider the possible negative effects of non pharmaceutical interventions, and (vii) to consider not only the public health benefits, but also the ethical, social, economic and logistical costs [63].

In addition to the IOM recommendations, our review has identified the following gaps in the academic literature: (i) there is a lack of comprehensive models for global spread of pandemic influenza, (ii) there is a lack of models which incorporate realistic travel networks and heterogeneity of the world regions, and (iii) there exists an important need to develop models which can quantify the impact of sharing mitigation resources between countries during global pandemic outbreaks.

The need to develop heterogeneous global pandemic models can be challenging due to the lack of centralized sources of data. Every country manages its own census data and publishes information in different formats or even sometimes refuses to share it with the international community. In this work, we are interested in in modeling the propagation of an outbreak born in a country with a high level of diversity in both the economical and social aspects. Mexico is the ideal candidate because: (i) it has both industrialized cities and extremely undeveloped regions, (ii) it is adjacent to the United States, (iii) it has a policy of sharing information with the international community and features a well developed national statistics system, and (iv) it was the first country to declare the H1N1/2009 outbreak which made apparent the lack of effective international surveillance and resource sharing policies.

3. Research Objectives

Our first research objective is to enhance capacity management strategies for multi-region pandemic surveillance. The global surveillance network has only a limited number of laboratories, most of them being located in developed countries, to perform surveillance in large populations. During an outbreak, the number of samples to process may become extremely large, and hence a capacity management problem can become a serious issue. To address this challenge, we formulate a capacity optimization model of a single lab surveying several geographical regions. The model can be extended to consider a network of labs that can share surveillance capacities.

Our second research objective is to estimate the outbreak propagation time from the onset to a likely pandemic export region, such as an international travel hub. For this purpose, we have adapted the simulation model developed by Uribe et al. [36] for the case of Mexico. Our testbed implementation features a set of regions with comprehensive consideration of social, demographic and economic attributes as well as a complex travel network that mimics travel patterns within Mexico.

Our third research objective is to examine different U.S. antiviral sharing strategies during global influenza pandemics. For this purpose, we experimented with different levels of surveillance, various non-pharmaceutical interventions (NPI) as well as antiviral stockpiles and prophylaxis and treatment strategies. We developed an empirical relationship to quantify the impact of various U.S. - Mexico resource sharing strategies under several pandemic detection and response scenarios.

4. Development of Optimal Capacity Management Strategies for Pandemic Influenza Surveillance

Before 2009, PI surveillance systems were focused on the H5N1 virus with emphasis on Southeast Asia. Due to the experience with H5N1 outbreaks in developing countries, U.S. labs were designed to deal with a low transmissibility and high severity virus. The H1N1/2009 outbreak demonstrated that the U.S. surveillance system was not prepared to handle a high transmissibility virus. Fortunately, H1N1 was not as severe as H5N1, but the number of specimens arriving to the labs at the peak of the outbreak caused significant processing delays. This issue brought attention to a capacity priority dilemma between diagnosis and surveillance functions of the labs.

In U.S., the main objective of the state labs is surveillance while diagnosis is mostly a function of the private labs. As the H1N1/2009 outbreak showed, at the beginning of an outbreak, private labs may not have the necessary materials to perform the appropriate tests. As a consequence, medical providers would have to send their specimens to the state labs for diagnosis confirmation. Even when the private labs become able to perform the tests, high processing costs or lack of confidence can result in additional diagnosis workload for the state labs. However, at this point of the outbreak, the priority should be shifted to surveillance. Normally surveillance is done using specimens sent by medical sentinel providers. In addition, diagnosis specimens can also contribute to the surveillance of a particular area. During the latest pandemic, most state labs operated under the "first come, first served" processing policy. As a result, when the number of specimens to be processed significantly exceeded the capacity of state labs, the lead time from specimen reception to test result increased dramatically.

The most significant capacity bottleneck during the H1N1/2009 outbreak was surprisingly not due to the processing equipment, but to the pre-processing of the specimens. Once a day, an unknown number of samples arrived to the lab, which then were tagged and recorded into the computer system by lab personnel. Little or no time was allocated for processing planning. Therefore, the "first come, first served" model made a lot of sense. After that experience, the state labs have been moving to using online specimen tracking systems. Such systems allow to have an advanced knowledge of the specimens in transit. However, the labs still lack effective planning mechanisms that will allow to improve the use of the limited capacity. This section develops such an optimization tool.

4.1 Single Lab Multi-Region Capacity Management Model

Figure 3 shows a schematic of the single lab multi-region model. We consider a single lab serving N potential outbreak regions over a surveillance horizon of T periods. During period r (e.g., one day), region i sends a number of specimen $Q_{ir} \geq 0$ to the lab. Each region i has a surveillance goal G_i, which is the number of specimens to process during the entire surveillance horizon. The lab has a finite processing capacity C_p during each period p. In each period r, when the lab receives a specimen, it must decide when to process this specimen (immediately or at a later time $r \leq p$).

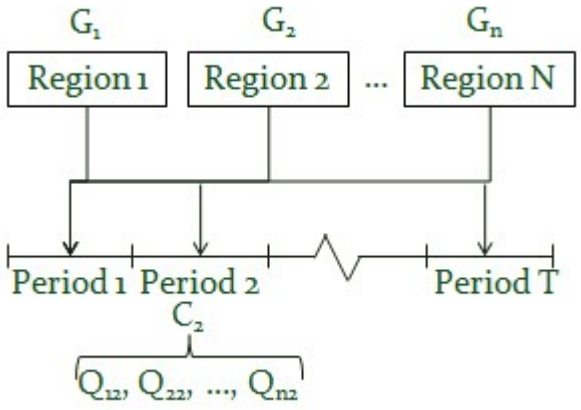

Figure 3: Schematic of the Single Lab Multi-Region Model

As an example, consider the Hillsborough county of the State of Florida (see figure 4). The county can be partitioned in a number of regions based on the zip codes. For each one of the regions (zip codes), a surveillance goal can be set, depending on the population of the region and the population density. The surveillance horizon can be one week, formed by seven daily periods. When sentinels or medical providers send specimens to the lab, it will aggregate the specimens by zip code for each period. For example, the specimens sent from region 3 during day 2 will be denoted Q_{32}. According to the specimens inventory remaining from the previous days, the available daily capacity, and the forecasted demand, the objective of our model is to decide how many specimens to process for both surveillance and diagnosis, for each region, during each period of the surveillance horizon. The decision criterion is minimization of the total penalty cost due to untimely surveillance and diagnosis processing.

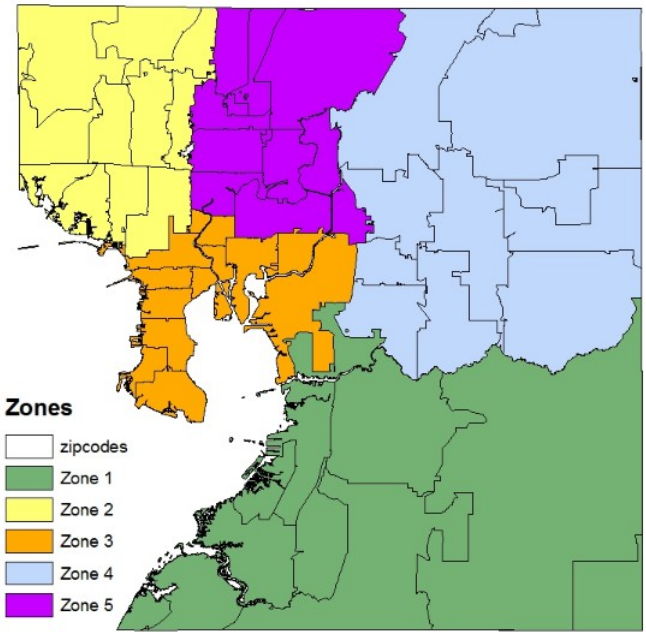

Figure 4: Hillsborough County with Zip Code Based Clusters

First of all, we need to introduce some notation:

N = number of regions served by the lab;

T = number of periods within the surveillance horizon;

C_p = total available lab capacity in period p;

Q_{ir} = total number of specimens received from region i in period r;

G_i = total surveillance goal for region i over the surveillance horizon ($G_i = 0$ if an outbreak has already been detected in region i);

π_S = penalty cost per unprocessed surveillance specimen;

π_D = penalty cost per unprocessed diagnosis specimen per period.

The decision variables are the following:

$S_{irp} \geq 0$ = number of specimens processed for surveillance of region i in period p from the specimens received in period r, $r \leq p$ ($S_{irp} = 0$ if an outbreak has already been detected in region i);

$D_{irp} \geq 0$ = number of specimens processed for diagnosis from region i in period p from the specimens received in period r, $r \leq p$.

The following linear programming model can be built:

$$\text{Minimize } z = \pi_S \sum_{i=1}^{N}(G_i - \sum_{r=1}^{T}\sum_{p=r}^{T} S_{irp}) + \pi_D \sum_{i=1}^{N}\sum_{r=1}^{T}\sum_{p=r}^{T}(Q_{ir} - \sum_{k=r}^{p}(S_{irk} + D_{irk}))$$

subject to:

$$\sum_{p=r}^{T}(S_{irp} + D_{irp}) \leq Q_{ir}, \text{ for all } i = 1, ..., N, \text{ for all } r = 1, ..., T \quad (1)$$

$$\sum_{r=1}^{T}\sum_{p=r}^{T} S_{irp} \leq G_i, \text{ for all } i = 1, ..., N \quad (2)$$

$$\sum_{i=1}^{N}\sum_{r=1}^{p}(S_{irp} + D_{irp}) \leq C_p, \text{ for all } p = 1, ..., T \quad (3)$$

The objective function minimizes the sum of the penalty costs due to untimely surveillance and diagnosis. The first term is the penalty cost due to unmet surveillance goals over all unaffected regions. The second term is the total penalty cost associated with delayed diagnosis of the specimens.

The problem is subject to the following sets of constrains. Constraints (1) account for the specimens received from each region during each period. Constraints (2) assure that the number of processed surveillance specimens cannot exceed the regional surveillance goal. Constraint (3) is the daily capacity constraint.

4.2 An Illustrative Example

To illustrate the use of the developed model, we considered a single lab monitoring four regions ($i = \{1, 2, 3, 4\}$), with respective weekly surveillance goals $G_1 = 50$, $G_2 = 30$, $G_3 = 20$, and $G_4 = 20$. The daily capacity of the lab was set to $C_p = 60$ for all daily periods. The values of Q_{ir} for all regions are shown in Table 3.

To estimate the value of π_S, we proceeded as follows. We first selected two time epochs (days) in the outbreak period, t_1 and t_2 ($t_2 > t_1$), which represented two alternative days of initiation of mitigation strategies. Then we used the simulation model described in Chapter 5 to calculate the total outbreak costs for each time epochs t_1 (respective cost c_1) and t_2 (respective cost c_2). The incremental cost $(c_2 - c_1)$ divided by the difference $(t_2 - t_1)$ was interpreted as the daily penalty cost due to the detection delay associated with untimely surveillance. Since we were interested in the cost per unit of surveillance specimen during a surveillance horizon π_S, we multiplied the ratio by the total number of periods (days) in the surveillance horizon divided by the surveillance goal. Hence, the value of π_S was estimated as:

$$\pi_S = \frac{(c_2 - c_1)}{(t_2 - t_1)} \cdot \frac{T}{G}$$

To estimate the value of π_D, we divided the incremental cost $(c_2 - c_1)$ by the increment in the number of visits to doctor during the same time period $(n_2 - n_1)$ divided by $(t_2 - t_1)$. The resulting expression was used as an estimate of the cost per unprocessed diagnosis specimen per daily period.

$$\pi_D = \frac{(c_2 - c_1)}{(n_2 - n_1) \cdot (d_2 - d_1)}$$

To calculate the values of π_S and π_D, we used the following simulation parameters: region 14, random seed 23, antiviral stockpile 260,000, antiviral strategy using contact tracing, and no NPI enforced. The values of t_1 and t_2 were set to $t_1 = 10$ and $t_2 = 30$ days. The resulting values of π_S and π_D were $\pi_S = 608,100$ and $\pi_d = 967$ ($c_1 = 236,432,380$, $c_2 = 444,923,837$, $n_1 = 9,726$, $n_2 = 20,725$, and $T = 7$).

The solution of the optimization model is shown in Tables 3 and 4. It can be observed that the model prioritizes the processing of surveillance specimens while minimizing the delay in processing of diagnosis specimens, subject to available daily capacity. The result of the model is a specimen processing schedule that can be implemented by the lab. The optimal solution resulted in the total penalty cost of \$1,229,057. As a comparison, the total penalty cost of the "first come, first served" policy was \$2,445,257.

Table 3: Results of the Example of Single Lab Model with Four Regions

Receiving Day	Processing Day (p)	Region							
		1 ($G_1 = 50$)		2 ($G_2 = 30$)		3 ($G_3 = 20$)		4 ($G_4 = 70$)	
$\sum_{i=1}^{4} Q_{i1} = 72$	$C_1 = 60$	$Q_{11} = 18$		$Q_{21} = 18$		$Q_{31} = 18$		$Q_{41} = 18$	
		S_{11p}	D_{11p}	S_{21p}	D_{21p}	S_{31p}	D_{31p}	S_{41p}	D_{41p}
	1	-	18	-	18	-	6	18	-
	2	-	-	-	-	-	-	-	-
	3	-	-	-	-	-	-	-	-
1	4	-	-	-	-	-	-	-	-
	5	-	-	-	-	-	-	-	-
	6	-	-	-	-	-	-	-	-
	7	-	-	-	-	12	-	-	-
$\sum_{i=1}^{4} Q_{i2} = 270$	$C_2 = 60$	$Q_{12} = 100$		$Q_{22} = 100$		$Q_{32} = 30$		$Q_{42} = 40$	
		S_{12p}	D_{12p}	S_{22p}	D_{22p}	S_{32p}	D_{32p}	S_{42p}	D_{42p}
	2	-	-	-	32	-	-	28	-
	3	-	-	30	-	8	-	12	-
2	4	-	6	-	6	-	-	-	-
	5	9	8	-	4	-	4	-	-
	6	41	-	-	-	-	-	-	-
	7	-	14	-	7	-	7	-	-
$\sum_{i=1}^{4} Q_{i3} = 54$	$C_3 = 60$	$Q_{13} = 24$		$Q_{23} = 10$		$Q_{33} = 10$		$Q_{43} = 10$	
		S_{13p}	D_{13p}	S_{23p}	D_{23p}	S_{33p}	D_{33p}	S_{43p}	D_{43p}
	3	-	-	-	-	-	-	10	-
	4	-	12	-	6	-	6	-	-
3	5	-	-	-	-	-	-	-	-
	6	-	-	-	-	-	-	-	-
	7	-	-	-	-	-	-	-	-
$\sum_{i=1}^{4} Q_{i4} = 54$	$C_4 = 60$	$Q_{14} = 24$		$Q_{24} = 10$		$Q_{34} = 10$		$Q_{44} = 10$	
		S_{14p}	D_{14p}	S_{24p}	D_{24p}	S_{34p}	D_{34p}	S_{44p}	D_{44p}
	4	-	6	-	6	-	6	-	6
4	5	-	-	-	-	-	-	-	-
	6	-	-	-	-	-	-	-	-
	7	-	-	-	-	-	-	-	-
$\sum_{i=1}^{4} Q_{i5} = 65$	$C_5 = 60$	$Q_{15} = 35$		$Q_{25} = 10$		$Q_{35} = 10$		$Q_{45} = 10$	
		S_{15p}	D_{15p}	S_{25p}	D_{25p}	S_{35p}	D_{35p}	S_{45p}	D_{45p}
	5	-	9	-	9	-	9	-	8
5	6	-	-	-	-	-	-	-	-
	7	-	-	-	-	-	-	-	-
$\sum_{i=1}^{4} Q_{i6} = 49$	$C_6 = 60$	$Q_{16} = 19$		$Q_{26} = 10$		$Q_{36} = 10$		$Q_{46} = 10$	
		S_{16p}	D_{16p}	S_{26p}	D_{26p}	S_{36p}	D_{36p}	S_{46p}	D_{46p}
6	6	-	5	-	5	-	5	-	4
	7	-	-	-	-	-	-	-	-
$\sum_{i=1}^{4} Q_{i7} = 48$	$C_7 = 60$	$Q_{17} = 18$		$Q_{27} = 10$		$Q_{37} = 10$		$Q_{47} = 10$	
		S_{17p}	D_{17p}	S_{27p}	D_{27p}	S_{37p}	D_{37p}	S_{47p}	D_{47p}
7	7	-	5	-	5	-	4	2	4

Table 4: Summary of Single Lab Model Example

Receiving Day	Region							
	1 $G_1 = 50 = \sum_{r=1}^{7}\sum_{p=r}^{7} S_{1rp}$		2 $G_2 = 30 = \sum_{r=1}^{7}\sum_{p=r}^{7} S_{2rp}$		3 $G_3 = 20 = \sum_{r=1}^{7}\sum_{p=r}^{7} S_{3rp}$		4 $G_4 = 70 = \sum_{r=1}^{7}\sum_{p=r}^{7} S_{4rp}$	
1. $\sum_{i=1}^{4} Q_{i1} = 72$	$Q_{11} = 18$		$Q_{21} = 18$		$Q_{31} = 18$		$Q_{41} = 18$	
$\sum_{i=1}^{4}\sum_{p=r}^{7}(S_{i1p} + D_{i1p}) = 72$	S_{11p}	D_{11p}	S_{21p}	D_{21p}	S_{31p}	D_{31p}	S_{41p}	D_{41p}
	-	18	-	18	12	6	18	-
2. $\sum_{i=1}^{4} Q_{i2} = 270$	$Q_{12} = 100$		$Q_{22} = 100$		$Q_{32} = 30$		$Q_{42} = 40$	
$\sum_{i=1}^{4}\sum_{p=r}^{7}(S_{i2p} + D_{i2p}) = 216$	S_{12p}	D_{12p}	S_{22p}	D_{22p}	S_{32p}	D_{32p}	S_{42p}	D_{42p}
	50	28	30	49	8	11	40	-
3. $\sum_{i=1}^{4} Q_{i3} = 54$	$Q_{13} = 24$		$Q_{23} = 10$		$Q_{33} = 10$		$Q_{43} = 10$	
$\sum_{i=1}^{4}\sum_{p=r}^{7}(S_{i3p} + D_{i3p}) = 34$	S_{13p}	D_{13p}	S_{23p}	D_{23p}	S_{33p}	D_{33p}	S_{43p}	D_{43p}
	-	12	-	6	-	6	10	-
4. $\sum_{i=1}^{4} Q_{i4} = 54$	$Q_{14} = 24$		$Q_{24} = 10$		$Q_{34} = 10$		$Q_{44} = 10$	
$\sum_{i=1}^{4}\sum_{p=r}^{7}(S_{i4p} + D_{i4p}) = 24$	S_{14p}	D_{14p}	S_{24p}	D_{24p}	S_{34p}	D_{34p}	S_{44p}	D_{44p}
	-	6	-	6	-	6	-	6
5. $\sum_{i=1}^{4} Q_{i5} = 65$	$Q_{15} = 35$		$Q_{25} = 10$		$Q_{35} = 10$		$Q_{45} = 10$	
$\sum_{i=1}^{4}\sum_{p=r}^{7}(S_{i5p} + D_{i5p}) = 35$	S_{15p}	D_{15p}	S_{25p}	D_{25p}	S_{35p}	D_{35p}	S_{45p}	D_{45p}
	-	9	-	9	-	9	-	8
6. $\sum_{i=1}^{4} Q_{i6} = 49$	$Q_{16} = 19$		$Q_{26} = 10$		$Q_{36} = 10$		$Q_{46} = 10$	
$\sum_{i=1}^{4}\sum_{p=r}^{7}(S_{i6p} + D_{i6p}) = 19$	S_{16p}	D_{16p}	S_{26p}	D_{26p}	S_{36p}	D_{36p}	S_{46p}	D_{46p}
	-	5	-	5	-	5	-	4
7. $\sum_{i=1}^{4} Q_{i7} = 48$	$Q_{17} = 18$		$Q_{27} = 10$		$Q_{37} = 10$		$Q_{47} = 10$	
$\sum_{i=1}^{4}\sum_{p=r}^{7}(S_{i7p} + D_{i7p}) = 20$	S_{17p}	D_{17p}	S_{27p}	D_{27p}	S_{37p}	D_{37p}	S_{47p}	D_{47p}
	-	5	-	5	-	4	2	4

5. Estimation of the Outbreak Propagation Time from the Onset to a Likely Pandemic Export Region (Testbed of Mexico)

It is believed that a new strain of PI will likely emerge in a rural area of a developing country [10]. Such areas typically have high population density and extreme poverty conditions leading to close and repetitive contact with animal reservoirs. In addition, such areas lack basic hygienic measures and have inadequate health care infrastructure. Because of historic reasons, most of the global surveillance systems and preparedness programs have concentrated their efforts on monitoring the Southeast Asia. As a consequence, the emergence of a new virus in rural Mexico in 2009 was somewhat unexpected. Since the virus was detected by observing changes in vital statistics and not by surveillance laboratories, the epidemiologists knew very little about the behavior of the novel virus strain. The result was the overestimation of its severity and the implementation of strict non-pharmaceutical interventions, causing significant economic costs. When the virus arrived to the U.S., the surveillance studies conducted by the CDC in Chicago and Delaware [64] made it possible to estimate the true potential impact of H1N1/2009. Consequently, the NPI implemented by the U.S. government were more proportionate to the virus severity.

The H1N1/2009 experience gave an important evidence of the lack of effective surveillance systems in most developing countries outside the SE Asia region. On the other hand, it takes six to nine months to develop and produce an effective vaccine in sufficient quantities to mitigate the impact of a PI outbreak. If the existing surveillance networks can be enhanced, more potentially harmful viruses can be included in the formulation of annual seasonal vaccines. Furthermore, additional information on the transmissibility and severity of new virus strains would be available before a

pandemic outbreak is born. If a new outbreak is detected early in an isolated region, the travel restrictions and antiviral prophylaxis (normally considered as ineffective intervention measures) may contain the pandemic at the source. Even if an outbreak cannot be contained, the possibility of decreasing its pace may give public health officials additional time for studying the virus, designing adequate containment policies, and starting production of a vaccine to face a second pandemic wave.

Our literature review has shown that such ideas are still hypothetical. A modeling environment where these hypotheses can be tested needs to be developed. We selected Mexico as a testbed for a variety of reasons including its recent pandemic history, its proximity to the United States, the availability of various types of data, our familiarity with its socio-economic structure, and the heterogeneity of its regions. It is indeed difficult to find a world region with some extremely undeveloped regions and high PI potential so close and so connected to the United States.

5.1 Regional Structure of Mexico

The country of Mexico is administratively divided into 32 states and 2495 municipalities (see Figure 5). Most of the economic and demographic data collected by the Mexican National Institute for Statistics, Geography and Informatics (INEGI) are reported either at the state or at the municipal level. However, from a modeling perspective, the states can be too large and heterogenous areas, making most of the modeling assumptions very aggregate and thus impractical. On the other hand, the municipalities are usually small areas, too numerous in quantity, and often possessing closely related characteristics with their bordering neighbors. Modeling the country at the municipal level will unnecessarily increase the model complexity and inevitable limit its computational feasibility. Therefore, we divided the states into homogeneous areas by aggregating the municipalities with similar characteristics and common borders. Such a cluster of municipalities within a state was defined as a region, the cell-unit used in our simulation.

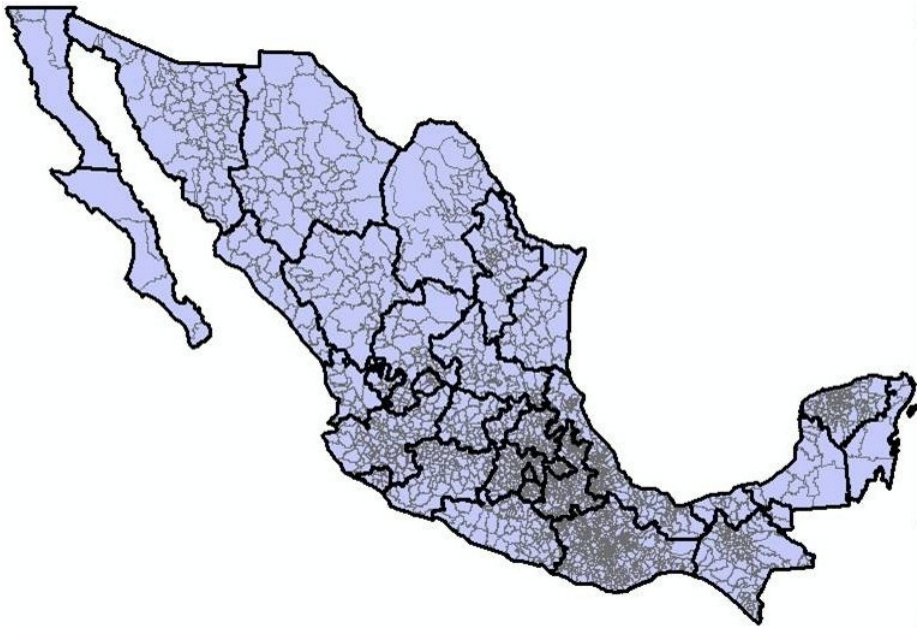

Figure 5: Administrative Structure of Mexico

In order to form the regions, we developed the following heuristic. The heuristic can be particularized to other countries with similar granularity of data. The heuristic is based on two rules: (i) a region has to be composed by municipalities (splitting municipalities is not allowed) and (ii) a region has to be completely within the borders of a state. We also tried to limit the average size of a region to 500,000 people.

The heuristic for region formation is presented below:

I. Set a regional population goal to S.

II. Select a state which has not been clustered. If none available, stop.

III. Start forming a new region

III.a Find an unassigned municipality with the highest population density in the state and assign it to the new region.

III.b If the region size is smaller than S and if there are unassigned municipalities in the state then,

III.b.i Add an unassigned municipality with the highest population density which is adjacent to the last added municipality. Repeat step III.b.

III.b.ii Otherwise, the formation of the region is complete. Go to step III.

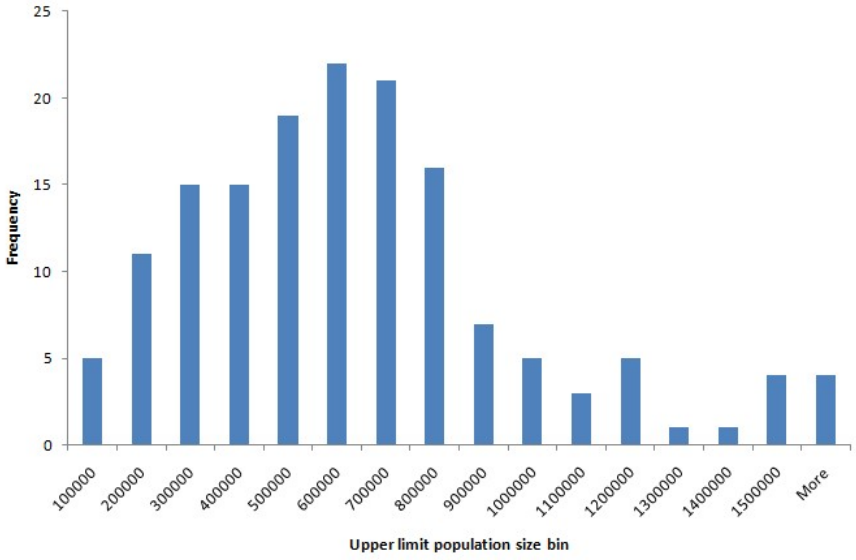

Figure 6: Histogram of the Size of the Regions Using the Developed Heuristic

Figure 6 shows the resulting histogram of the size of the regions applying the described heuristic. At the end, it was decided to make an exception for the case of Mexico City and model it as a single region of 19.25 million people. Without considering Mexico City, the regional population size averaged 600,234 individuals with a median of 548,794, a standard deviation of 365,611, a minimum value of 54,792 and a maximum value of 2,145,452. The procedure resulted in a total of 154 regions plus Mexico City (see Figure 7).

INEGI reports the data on demographics, household distributions, health services, and school systems at the state level [65], while workplaces and population size are reported at the municipal level [66]. Consequently, certain levels of (des)aggregation were needed to organize the data for each of the regions. To this end, it was necessary to filter, query, and merge data from several databases using SQL. The original format of the raw data was converted to the format shown in Appendix C.

At the end of this section, we can note from our experience that the main obstacle that modelers may face when developing systems like the one we are describing will likely be the lack of a universal data format followed by all countries in the way they report demographic, economic, transportation, and healthcare related information.

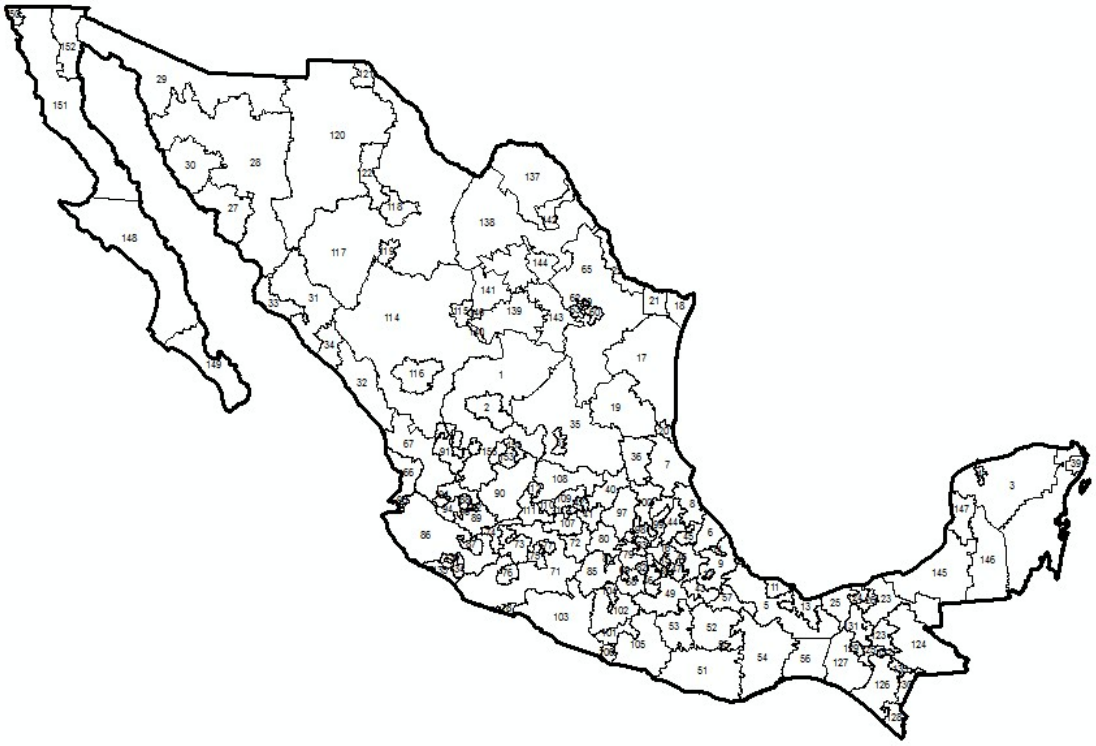

Figure 7: Mexico Partitioned into 155 Regions

5.2 Likely Pandemic Export Regions

Table 5 suggests that once an outbreak has started in Mexico, it is very probable that it would be exported abroad by a foreign visitor rather than a Mexico resident [65]. Because of this consideration, a certain number of regions would more likely be responsible for pandemic export. These regions, called likely pandemic export (LPE) regions, include major transportation hubs and the regions with a common border with the U.S. (see Table 6 and Figure 8). It can also be noted from Figure 8 that the United States attracts 77% of all Mexican abroad travel [67].

Table 5: International Travel to/from Mexico

Total visits (2008):	26.2 M	
Foreign travelers	21.6 M	(82.5%)
Tourists	10.5 M	(40.0%)
Cruises/sea commerce	8.1 M	(31.0%)
Business/others	3.0 M	(11.5%)
Mexicans	4.6 M	(17.5%)

Table 6: Areas of Mexico with Major International Transportation Hubs

Area [number of regions]	Travelers	
Quintana Roo (Cancun) [1]	9.1 M	(35%)
Mexico City [1]	5.0 M	(19%)
Jalisco (Guadalajara, Puerto Vallarta) [2]	3.0 M	(11%)
Baja California Sur (Los Cabos) [1]	2.3 M	(8.5%)
Border States (6 States) [14]	2.8 M	(11%)

By analyzing the recent pandemic history, it can be expected that a PI outbreak is very likely to originate from an isolated and economically underdeveloped rural area. At the outbreak onset, the probability of an immediate global spread is small because of the geographic isolation of the region. It is when the outbreak reaches one of the LPE regions shown in Figure 8 that the probability of a global outbreak substantially increases. Then the following questions arise: (i) How long does it take from the onset of the outbreak until it reaches one of the LPE regions? (ii) Is it possible to contain or slow down a global outbreak if the virus is promptly detected in the originating areas? (iii) What mitigation resources are needed to achieve these goals? (iv) What type of surveillance system is required for a timely pandemic detection? (v) Would developed countries, namely the U.S., be willing to share the required resources to avoid or mitigate global outbreaks?

To the best of our knowledge, it is not possible to answer the above questions with the existing models. It is therefore the main motivation of our work to try answering these questions to the best of our ability.

5.3 Designation of Economically Undeveloped Regions

In order to determine economically undeveloped regions, we have used the data on the social security coverage rather than the unemployment rate. The reason for that is due to the fact that because of its traditional definition in the economic sciences, some of the economically undeveloped states can have a relatively low unemployment rate [68]. There are two major public health institutions in Mexico which provide

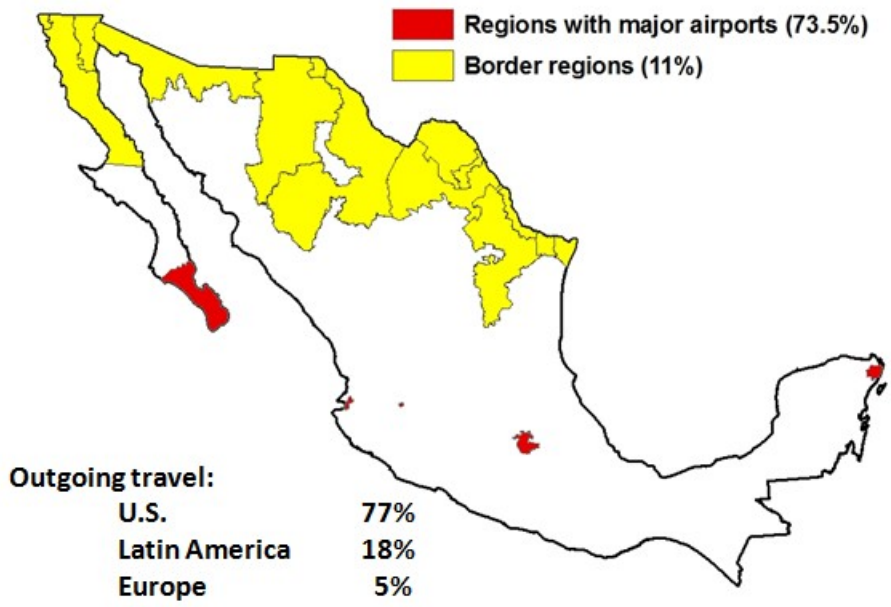

Figure 8: Likely Pandemic Export Regions in Mexico

medical insurance to workers, their economic dependents, and retirees. These institutions are the Mexican Institute of Social Security (IMSS) with 49.1 M beneficiaries and the Institute of Security and Social Services of State Workers (ISSSTE) with 11.1 M people covered [69]. For an employed Mexican resident, it is mandatory to pay insurance premiums to one the above institutions. Consequently, the residents without a formal job are not covered by these organizations. Both IMSS and ISSSTE report state level statistics in the form of the ratio of insured population to the total population of the state. In our testbed, we selected economically undeveloped regions from the states with the ratio less than or equal to 0.5. As a result, we have selected 69 potential outbreak starting regions in the following states: Chiapas (the ratio is 0.25), Oaxaca (0.31), Puebla (0.36), Tlaxcala (0.38), México (0.38), Guerrero (0.39), Hidalgo (0.41), Tabasco (0.42), Veracruz[1] (0.42), Michoacán (0.45), and Morelos (0.49). It can be observed from Figure 9 that the economic undeveloped regions are mostly concentrated in the central and southern part of the country.

[1]The first cases of the H1N1/2009 were reported in the Mexican state of Veracruz [54].

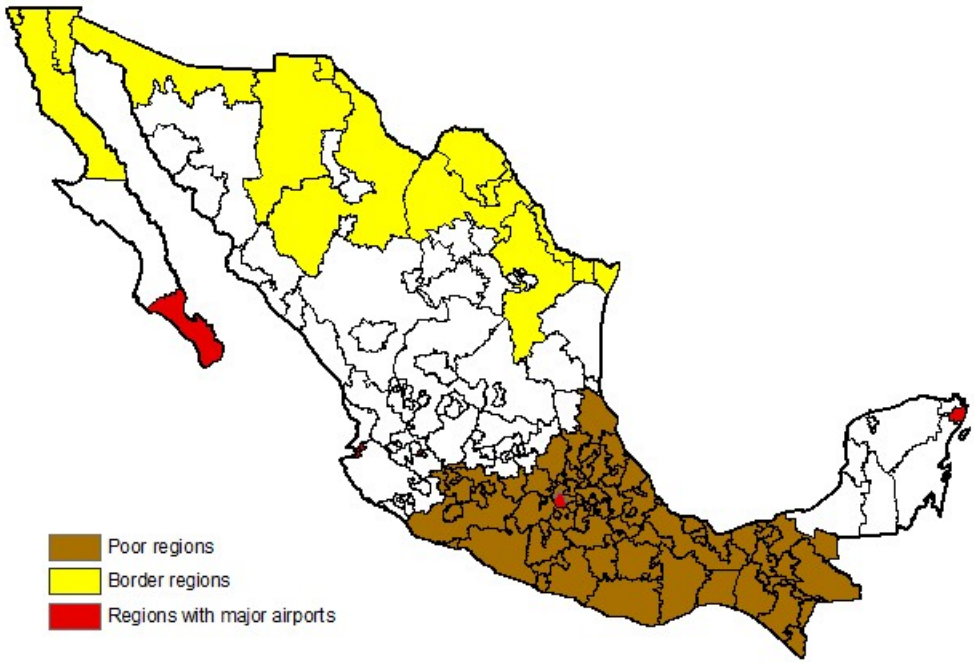

Figure 9: Economically Underdeveloped Regions and LPE Regions in Mexico

5.4 Multi-Region Travel Network

Most papers on modeling global spread have used air travel as the only mode of transportation for the population under study [28, 38, 43]. However, as it can be seen from Table 7, a travel model for Mexico needs to take into consideration the land transportation because it accounts for 97.7% of the domestic travel volume [70]. On the other hand, air transportation accounts for only 1.6%. However, air transportation will likely play a key role in potential export of a PI outbreak.

Table 7: Distribution of Domestic Travel by Transportation Mode

Transport Type	Percentage
Highways	97.7%
Air	1.6%
Railroads	0.3%
Sea	0.4%

In order to determine the inter-regional travel probabilities, we adopted a database that listed the geographic location and aggregated demographic information of 4,400 urban areas of Mexico [71]. For the purposes of our model, we selected the largest

urban areas/cities which were most representative of each of the 155 regions discussed in Section A. A total of 164 cities were selected (they are represented by green dots were selected which are in Figure 10, left).

One of the biggest challenges we have encountered was to connect the selected cities in a way that would mimic the land transportation network of the country. Data from the three largest bus companies in the country were obtained from their web pages [72–74]. With that information and the data obtained from the Mexican Institute of Transportation [67], we estimated the traffic volume between the regions by using the daily number of buses that cruised between the respective cities of the regions (see Figure 10, right). Using these data, we obtained an origin/destination traffic volume matrix which was transformed into a 155x155 matrix of inter-regional travel probabilities.

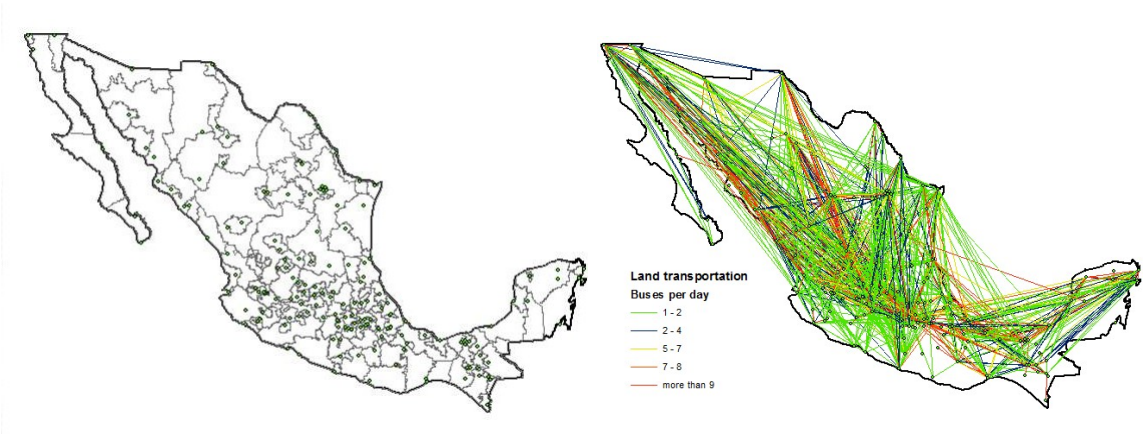

Figure 10: A Schematic of Inter-Regional Traffic Volume Network

According to the Mexican Institute of Transportation, the probability of a Mexican resident traveling outside his community is 8% on any given day [70]. However, it should be noted that in that study communities are defined as areas located in close geographic proximity. As a consequence, the above probability would also include internal travel within our testbed regions and thus should only be used as an upper bound. Longini et al. used a daily travel probability of 1% in the case of Thailand [16]; this value was also used in our model.

5.5 Multi-Region Pandemic Simulation Model

Appendix B shows a schematic of the multi-regional simulation model developed by Das et al. [35]. The agent-based simulation model mimics the detailed social and disease dynamics, featuring hourly schedules of regions inhabitants while they work or attend school, run errands, attend leisure activities, or stay at home with their families. The simulation was developed in C following an object-oriented programming style. In the following paragraphs, we will explain the main functions of each object or subprograms to give the reader a better understanding of the simulation structure. This simulation has been published in the academic literature [35, 75].

The object *Main* controls the simulation. *Main* declares all the constants and calls the following objects in a sequential order: *Read Input, Initialize, Ongoing Region, Cost, Daily Statistics,* and *Reproduction Number*. The first two objects are called once at the beginning of the simulation, whereas the others are called on a periodic (daily or hourly) basis. *Main* also determines the maximum duration of the simulation and records the daily statistics in the respective output files.

Read Input reads a set of input files and assign values to most simulation variables. Since every region has different demographics, different data is needed to capture the heterogeneity of the regions. Appendix C lists the different read files and their structure. *Read Input* opens each one of the files, declares arrays of appropriate sizes, writes the input data into the arrays, and closes the input files. Most of the constants are declared within the main simulation program. However, if they need to be modified, *constants.txt* is the input file that contains their values. Additionally, *constants.txt* indicates which region need to be simulated and which random replication seed will be used. When an experiment is designed, different simulation versions will use different versions of the *constants.txt* file.

After calling *Read Input*, *Main* calls *Initialize*. *Initialize* creates an array of regional variables that will be updated during the simulation, and then calls *Generate*

Businesses and *Generate Entities*. *Generate Businesses* creates a set of business structures to designate workplaces of individuals. Additionally, the object also declares mixing groups within businesses structures of the region. *Generate Entities* creates individual (human) entities, assigning them a particular household. In addition, each individual is assigned a set of attributes that will be tracked and updated during the simulation. After creating an adult entity, the simulation calls *Adult Age Workplace*, whereas after creating a child entity *Children Age School* is called. These objects assign adults and children to their respective workplaces/schools, mixing groups, and after-school activities.

Once the regional community has been generated, *Main* calls *Ongoing Region*. After initializing the vector value of daily statistics, it checks if the outbreak has started in the region, and then calls *Generate Outbreak*. *Generate Outbreak* randomly selects a pre-defined number of initial infected individuals from the regional population and starts their disease clock. After that, *Ongoing Region* checks the status of NPI in the region and calls the appropriate scheduling object. Schedules are created on an hourly basis so that each individual is situated in a particular establishment at any moment during the simulation. Then *Disease Progress, Tracking Individuals, Household Spread, Hourly Contact*, and *Visit Doctor* objects are called every hour.

Disease Progress monitors all infected individuals within a region. Every hour, the disease clock of each infected individual is updated until a culmination period is reached. At this point, the individual either recovers or dies with some probability. *Recover Process* records the statistics of the recovered individuals by age in the output files. Recovered individuals develop full immunity. *Disease Progress* also calculates the mortality probability based on the age based mortality probability and status of antiviral treatment. *Death Process* collects the statistics of the deceased individuals.

Every business entity in the simulation is divided into mixing groups, allowing individuals to have a closer interaction with others in their respective mixing group.

Tracking Individuals creates two tracking arrays within a mixing group, one for susceptible individuals and one for infected individuals. Every time an individual is infected, he is moved from the susceptible array to the infected array. When an individual dies, he is removed from the respective mixing group. When an individual recovers, he remains in the mixing group, but is removed from the susceptible and infected arrays. *Tracking Individuals* also counts the number of susceptible households at any point during the simulation.

Household Spread tracks the contacts among susceptible and infected individuals within each household. Each hour, the object checks who is present in the household and creates random (uniform) contacts. For any new contacts, *Household Spread* calls *Infection*. *Hourly Contact* is the analogous object for businesses. It checks the contact among infected and susceptible individuals within mixing groups. Contact rates vary with business type. *Household Spread* and *Hourly Contact* calculate duration of contact Δt for each contact event. *Infection* calculates the probability of infection for each susceptible contact. *Visit Doctor* handles the individuals who are looking for medical assistance. Additionally, it administers antiviral drugs according to a preset policy, and declares social distancing strategies (individual, household, workplace, or community based).

At the end of each day, the main program checks if there are N infectious travelers in any of the unaffected regions. If so, the program starts running the new outbreak(s) in parallel with the rest of the ongoing outbreaks. This process is sketched in Figure 11. The main simulation ends when an outbreak reaches a likely export region, or if the outbreak is contained no more infected individuals are generated before reaching such a region. The maximum simulation duration was set to 600 days.

Three additional objects are called to calculate the daily statistics. *Cost* computes the cost due to deaths, hospitalized individuals, and loss of productivity. While it is difficult and polemic to attempt translating human life into money, it is nevertheless

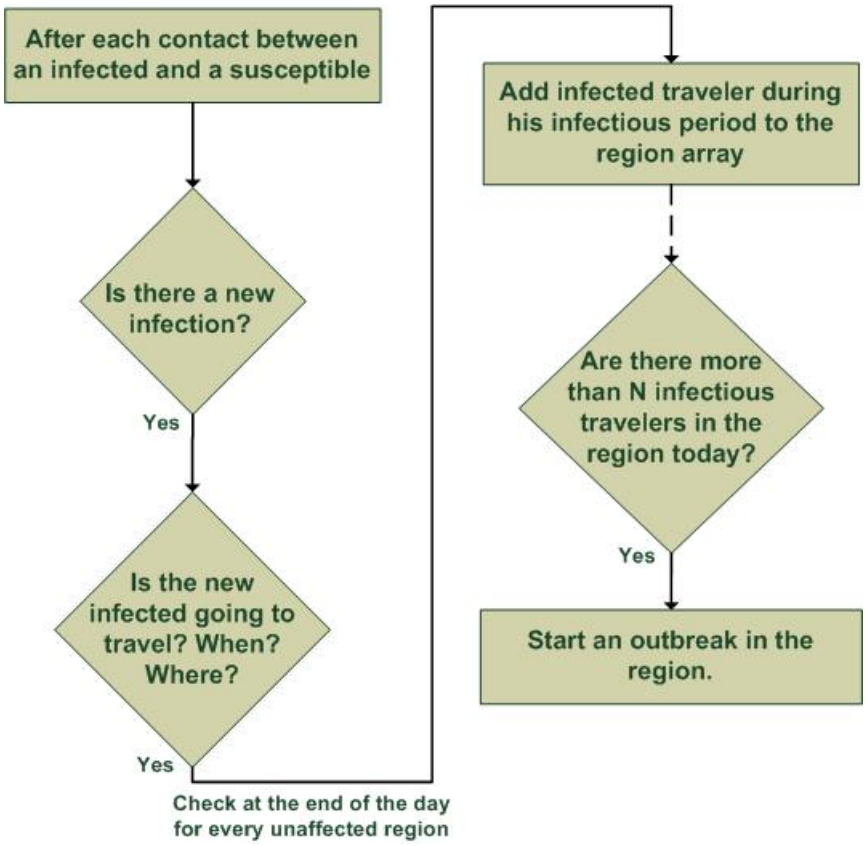

Figure 11: A Schematic of a Regional Outbreak Generation

necessary to have a common unit to measure the aggregated impact of death, loss of productivity, and medical expenses. Besides, we only used the cost criterion to compare different simulation scenarios. *Daily Statistics* records daily information in the output files *SummaryRegion.txt* and *ContactProcess.txt*, while *Reproduction Number* takes care of the statistics by generation of infected in the file *ReproductionNumber.txt*. The content of these output files is listed in Appendix C.

5.6 Automated Replication Interface

Our multi-region simulation model is programmed in C. Because it was required to run the model thousands of times with different parameters, we developed an automated replication program using Visual Basic Applications (VBA). We used MS Access to define an experiment as a table. Such an experiment is composed of several simulations, all of them with different parameters. A client computer inquires the

database for any simulations to be run, in which case the VBA program creates the input files with the parameters taken from the table. Every client computer is connected to the server and independently runs the simulations and generates the output files. When the simulations finish, the VBA program reads and records the output files in the central database. Using the database, a comprehensive repository of results is created in MS Access, which can be organized and presented according to the needs of a decision maker. For more advanced statistical analysis, we used SQL to export a particular dataset to the SAS statistical software.

The automated replication program allows the end user to: (i) manage an experimental design of multiple scenarios, (ii) run automatically every simulation within a scenario, and (iii) create a repository of the results obtained from each simulation. We created a *Scenario Manager* using MS Access as the main tool to implement function (iii) and the VBA program to implement functions (i) and (ii) (see Appendix D).

Since all information obtained through the output files is read and stored in *Scenario Manager*, generic reports and graphs can be designed for each simulation and scenario. Figure 12 shows an example of the type of graphs that can be easily created. In this particular example, an outbreak starts in region 71 on day 1. On approximately day 35, two outbreaks start in regions 77 and 110, respectively. By day 75, the outbreak in the original region has reached its peak, but it is in an increasing stage in the other two regions. Another outbreak starts in region 30 around day 79. At day 86, an outbreak starts in region 96, a likely pandemic export region. At this point, the simulation ends.

5.7 Classification of Regions for Calibration Purposes

Mexico is a country with a very strong economic stratification, including one of the largest cities in the world with around 20 million people, some very industrialized and developed urban centers, small towns supported by family-owned businesses, tourist resorts with large hotels and casinos, and isolated rural areas where more

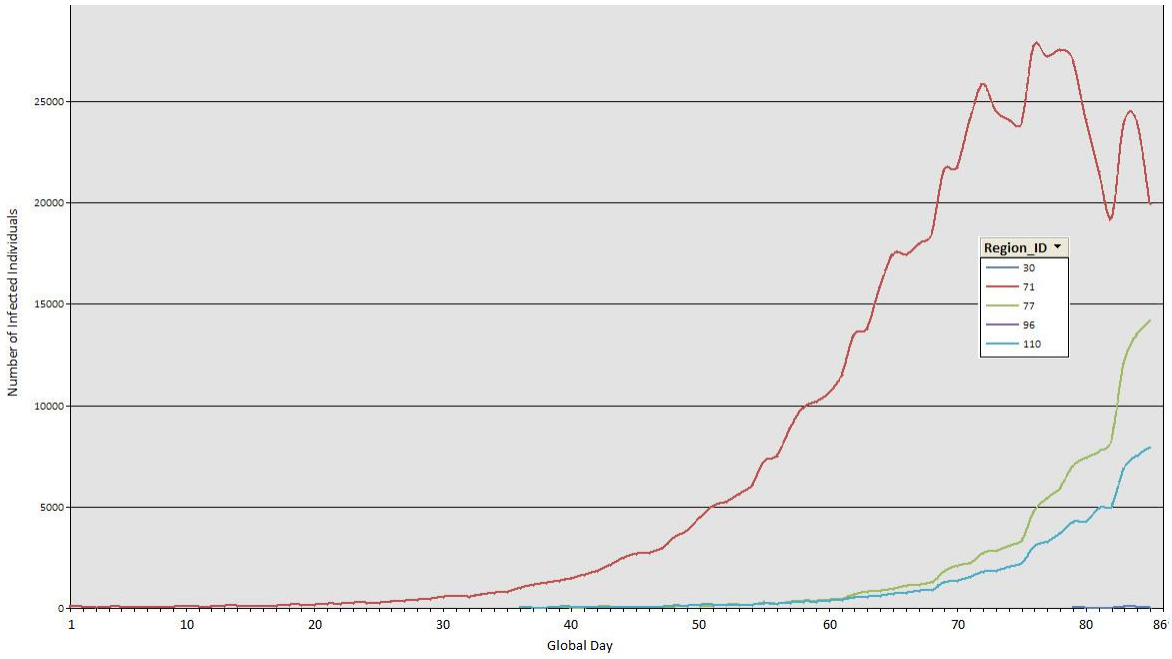

Figure 12: Example of a Graph Showing the Regional Daily Infection Rate

than 40 million people live under the conditions of extreme poverty. According to the census data, 95% of the Mexican companies have 5 employees or less [66]. However, the presence of large companies in certain regions may affect the way disease spreads. Because of this heterogeneity, in order to calibrate our simulation model, we classified all 155 regions into four quadrants, as shown in Figure 13. The x-axis presents the percentage of industrial businesses in the region, while the y-axis represents the average company size. The quadrants are divided by the mean value of each one of these variables. Detailed information for each region is presented in Appendix A.

5.8 Calibration of the Simulation Model

To calibrate our simulations for each quadrant, we used the disease strength parameter ρ. It has been observed from preliminary analysis that when using low values of ρ, a regional outbreak could be initiated and sustained using certain random seeds, but not the other seeds. A total of more than two thousand simulations were run to find the minimum value of ρ that would guarantee a sustained outbreak in each region. The details of the calibration results are presented in Appendix E. Table 8

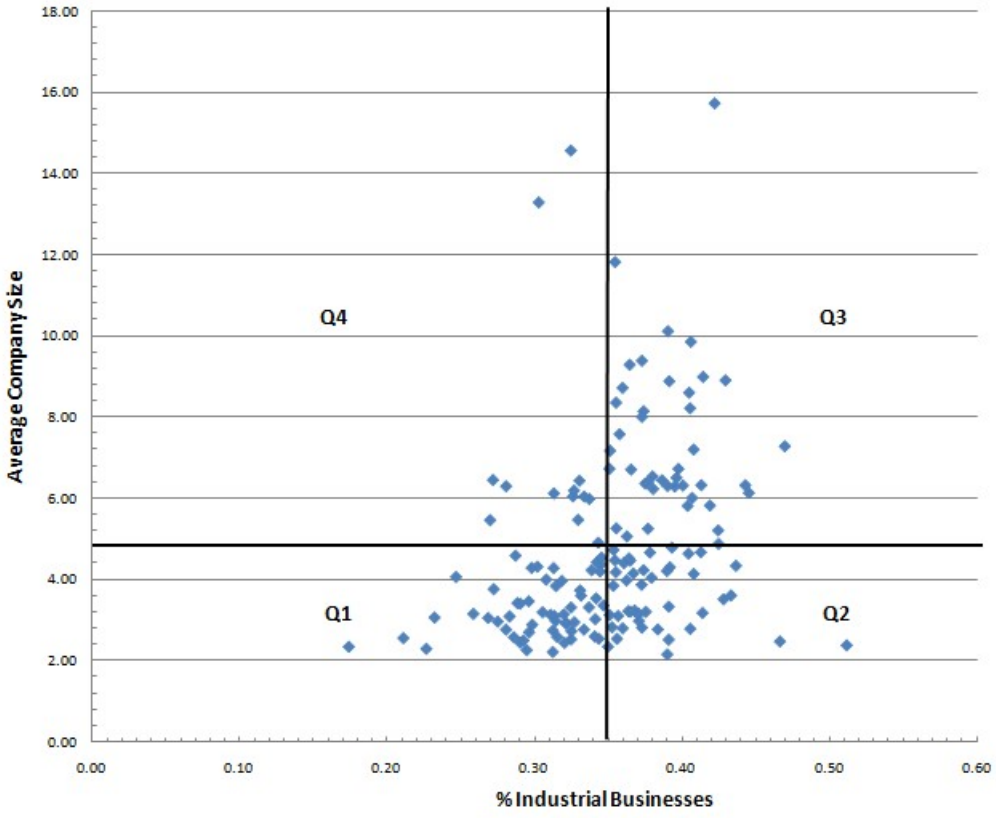

Figure 13: Regions Classified by Company Size and Percentage of Industries

summarizes the minimum values of ρ obtained from the calibration process and the percentages of the regions where an outbreak was able to be initiated and sustained.

5.9 The Outbreak Lead Time from the Onset to a LPE Region

To create a baseline scenario, we used the travel probability of 1%, as in Longini et al. [16]. We also adapted key parameters from Ferguson [28], such as a 27% initially immune population, 10 seed infectious to start a regional outbreak, and the value of $\rho = 1575$, to guarantee that an outbreak is started and sustained in any region, independently of the selected replication seed. We also used N=10 as the minimum number of infectious travelers in a region to declare an outbreak in the region.

We designed a preliminary experiment to estimate the impact of both the number of travelers to start an outbreak and the travel probability on the outbreak lead time. As initial regions, we used the sixty nine economically undeveloped regions defined

Table 8: Summary of Calibration Values of ρ

Minimum value of ρ	Number of Regions with Sustained Outbreaks	Cumulative % of Regions with Sustained Outbreaks	Total Population Size	Cumulative Population Size (% of Individuals)
975	1	0.6%	456,488	0.5%
1025	1	1.3%	718,103	1.3%
1100	53	35.7%	27'869,746	33.3%
1175	46	65.6%	27'520,549	64.9%
1250	23	80.5%	16'521,772	83.9%
1325	20	93.5%	8'578,487	93.8%
1375	6	97.4%	3'230,871	97.5%
1575	4	100.0%	2'195,718	100.0%

earlier in Section V.B (see Appendix C). We ran each initial region, one at a time, with the values of the travel probability 0.5% and 1%, and the number of travelers to start an outbreak of 5 and 10, with a total of 276 simulations. Table 9 shows the average lead time (in days) and the number of times each LPE region was reached.

From the table, it can be observed that in 84% of the time, the LPE region reached was a major city, either Mexico City (65%) or Guadalajara (19%). The U.S. border regions were reached in only 11% of the time, and the tourist regions were reached only 5% of the time. Only 11 out of 19 LPE regions were reached. The rest of the regions (65, 117, 120, 137, 138, 142, and 151) are underpopulated regions in widely arid areas, and region 149 (La Paz/Los Cabos) is geographically isolated from the rest of the country because of its location in the Baja California peninsula. Table 9 also shows that both the travel probability and the number of individuals to start an outbreak can affect the lead time. A more detailed analysis of the effect of these and other parameters on the lead time is developed in the next chapter.

Table 9: Summary of the Results for the Baseline Scenario

		Average Lead Time in Days (# Times Reached)	
Likely Pandemic Export Region	Travel Probability	# Individuals to Start an Outbreak 5	10
79. Ciudad de México, D.F.	0.5%	44.81 (44)	55.32 (46)
	1%	41.53 (45)	46.59 (44)
96. Guadalajara, Jalisco	0.5%	55.83 (12)	70.42 (14)
	1%	45.25 (12)	57.8 (15)
39. Cancún, Quintana Roo	0.5%	60.25 (4)	70 (2)
	1%	54 (4)	62.5 (2)
152. Mexicali, Baja California	0.5%	55.5 (4)	-
	1%	38.5 (2)	54.67 (3)
22. Nuevo Laredo, Tamaulipas	0.5%	37 (1)	46 (1)
	1%	47.5 (2)	55 (2)
21. Reynosa, Tamaulipas	0.5%	55 (2)	41 (1)
	1%	28.5 (2)	-
150. Tijuana, Baja California	0.5%	48 (1)	-
	1%	43 (1)	59.5 (2)
29. Nogales, Sonora	0.5%	52 (1)	-
	1%	41 (1)	49 (1)
18. Matamoros, Tamaulipas	0.5%	44 (1)	-
	1%	-	47 (1)
95. Puerto Vallarta, Jalisco	1%	31 (1)	41 (1)
121. Cd. Juárez, Chihuahua	1%	-	65 (1)

6. U.S. Resource Sharing Strategies During Global Influenza Pandemics

6.1. Mitigation Resources and International Collaboration

In Chapter 1, we discussed the importance of international collaboration to enhance the U.S. preparedness for a global pandemic outbreak. However, at present there exist no studies which can quantify the impact of collaboration, particularly resource sharing. Assigning too few resources to an international partner may not be enough to enhance our preparedness. On the other hand, sharing too many resources may be a costly enterprise which can undermine domestic preparedness and response. An adequate strategy would be the one that can increase the safety level of all involved countries by reducing the number of affected regions, increasing the lead time to allow manufacturers to produce more antiviral drugs and develop a potent vaccine, or even possibly containing the outbreak at the source. We explore diverse resource sharing strategies in this chapter.

Every resource sharing strategy has a probability of success and a cost and the decision makers have to balance these two factors. Our work attempts to provide public health officials with a decision aid model aimed at improving the existing ad-hoc resource sharing strategies during global influenza pandemics. In what follows, we discuss both pharmaceutical and non-pharmaceutical resources that can be shared with a country of pandemic origin.

Assuming the outbreak is caused by a novel virus strain, the only pharmaceutical mitigation resource available at early pandemic stages would be antiviral drugs. Currently, antiviral drugs are available in most pharmacies with a physician's prescription. However, a massive pharmaceutical prophylaxis will require substantial stockpiles and advanced distribution logistics. In this work, we are considering two

main factors that may affect the effect of antiviral-based intervention: antiviral distribution strategy and antiviral stockpile.

We consider three different antiviral distribution strategies. The first strategy prescribes antivirals to every symptomatic individual who visits a doctor. It can be noted that during the H1N1/2009 outbreak, the Mexican government was conservative about the use of antivirals and only provided them to the patients whose life was considered to be at risk. A risk adverse decision maker may adopt such a strategy in an attempt to avoid mutation of the virus into an antiviral-resistant strain. However, we will adopt a risk-neutral strategy and provide a complete treatment to every individual visiting a doctor. Our second strategy is based on contact tracing. In this case, not only the symptomatic individual receives the antiviral course, but also his/her household members as well as the members of his/her workplace mixing group. Because antivirals reduce the capability of the virus to reproduce in the human body, such a strategy may reduce both the infectiousness of infected cases and the exposure of uninfected individuals. Our third strategy attempts to provide antivirals to the entire regional population. We call this strategy 'blanket' since it attempts to cover an entire geographic region. In all strategies, the application of antiviral drugs was paced according to the available distribution capacity. Such a gradual distribution was particularly important for implementing the blanket strategy.

To implement an antiviral strategy it is necessary to have an adequate antiviral stockpile. Some of the above strategies require more courses than others, which may require the use of shared quantities. In this work, we studied how different levels of antiviral stockpile impact the effectiveness of a antiviral strategies.

We also consider certain non-pharmaceutical interventions which can be used by the Mexican authorities. During an outbreak, officials may decide to totally or partially close schools and workplaces and/or ban or limit public gatherings in places like theaters, stadiums, and churches. In 2009, the Mexican government was strict in

implementing non-pharmaceutical strategies, declaring closures of schools, non-vital workplaces, and banning social gathering for several weeks. These measures were implemented nationwide, even in unaffected regions. In our study, we only considered two scenarios when either most comprehensive, all inclusive NPI were implemented or when no NPI were used. By doing so, we sought to understand the isolated effect of non-pharmaceutical interventions on the outbreak lead time.

A variable that indirectly measures the efficiency of a surveillance system is what we called the detection delay. A sophisticated surveillance system is costly, but it can assure a fast detection and prompt intervention (pharmaceutical and non-pharmaceutical), while a nonexisting or inefficient surveillance system may reduce the intervention effectiveness because the outbreak has already spread to several regions. It can be noted that in the case of H1N1/2009, the outbreak was detected through vital statistics which showed an increase in the number of deaths due to respiratory diseases in certain regions. In this case, several weeks had elapsed from the onset of the outbreak until the emergency was declared.

From the perspective of a U.S. decision maker, understanding how the above factors affect the lead time of an overseas-born outbreak can be of significant importance. Knowing which factors and their levels are more relevant can aid in developing intelligent resource sharing strategies. The following analysis aims to achieve this goal.

6.2 Design of Experiment for the Outbreak Lead Time

After identifying the factors that can impact the outbreak lead time, we designed an experiment to quantify the impact through an empirical relationship. Table 10 summarizes the design of experiment. We selected six initial outbreak regions from different parts of the country with diverse population strata and economic development. The economic development was reflected in the quadrant of the region. Economically undeveloped regions tend to be located in quadrants 1 and 2, while heavily industrialized regions tend to be situated in quadrants 3 and 4. We selected

three levels of antiviral stockpiles: zero (none), a relatively small stockpile (260K), and a stockpile large enough to cover the entire population of the initial region and some more, if needed (2M). The stockpile was measured in terms of courses of doses. We used the three types of antiviral distribution strategies and the two types of non-pharmaceutical interventions described in the previous section. Finally, we used three levels of detection delay (1, 10, and 30 days) and three levels of N, the number of infectious individuals required to start a regional outbreak ($N = 3, 6$, and 10).

Table 10: Design of Experiment: Factors and Levels

Factor	Definition	# of Levels	Level Values					
-	Region ID	N/A	71	130	14	36	32	145
Q	Region quadrant	4	1	1	2	2	3	4
P	Population (in thousands)	6	931	195	482	646	620	378
N	Number of infectious individuals required to start a regional outbreak	3	3 6 10					
AS	Antiviral stockpile, courses	3	0 260,000 2,000,000					
AD	Antiviral distribution strategy	3	Treatment of visits to doctor (1) Contact tracing treatment (2) Blanket prophylaxis (3)					
NPI	Level of NPI	2	None (0) Comprehensive (1)					
D	Detection delay, days	3	1 10 30					

Figure 14 (top) illustrates the selected initial outbreak regions: four regions from quadrants 1 and 2, and two regions from quadrants 3 and 4, respectively. The regions also represented diverse geographic areas of the country (See Figure 14 (bottom)).

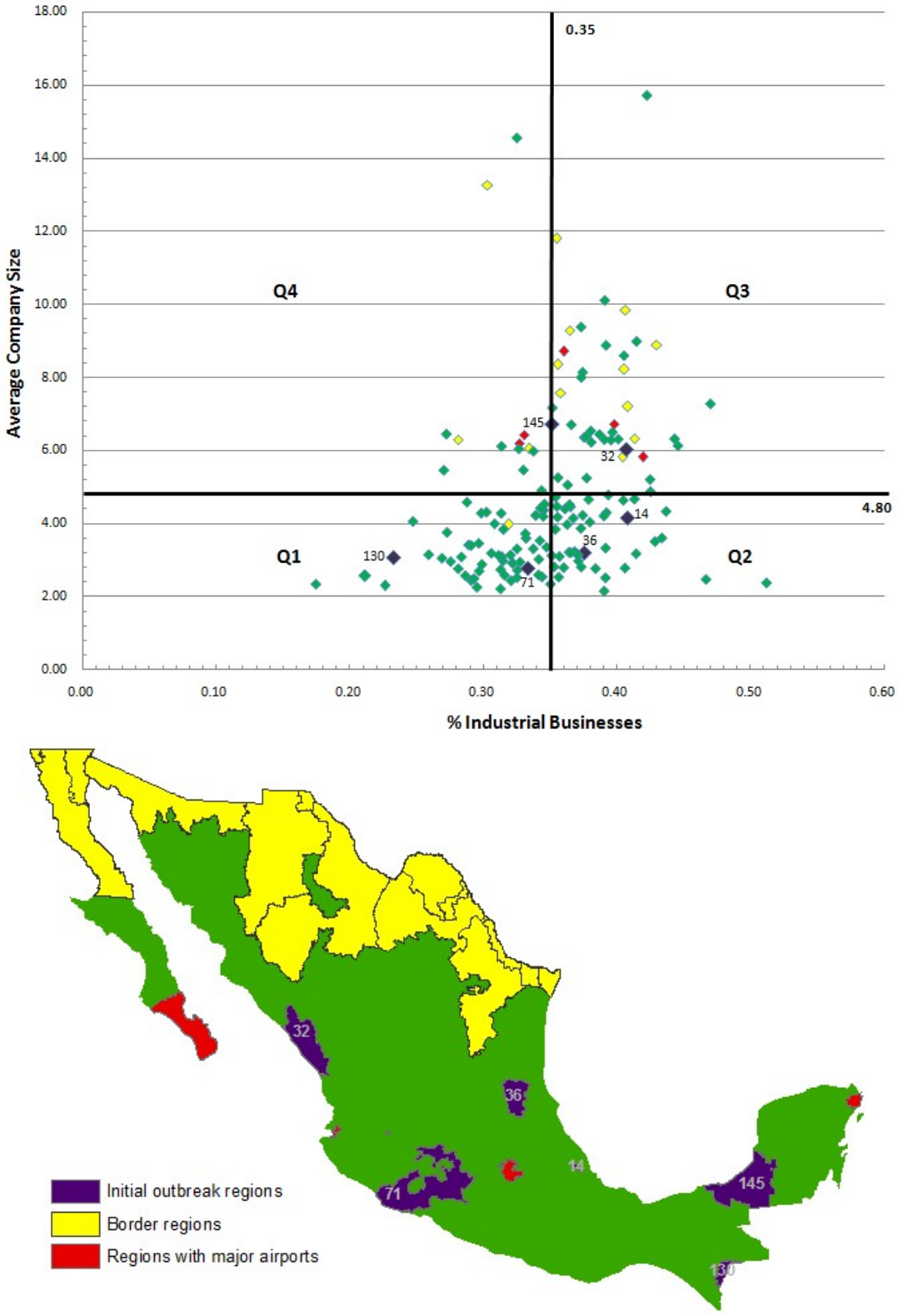

Figure 14: Regions Selected for the Design of Experiment

6.3 Empirical Relationship for the Outbreak Lead Time

We executed a total of 2,250 replicates using all possible combinations of the factor levels with three random replication seeds. The dependent variable was the outbreak lead time, defined as the number of days since the onset of the outbreak until it reaches a LPE region. We used SAS v.9.2 for the statistical analysis. The first statistical analysis we performed was a set of normality tests (see Appendix H).

To study the effect of the interactions among the factors, we used a regression model with the main factors and their second and third order interactions. We obtained a value of $R^2 = 0.7158$. However, some of the factor interactions were not significant. We eliminate from the model factor interactions with $p - values \geq 0.05$ and ended up with a value of $R^2 = 0.7028$ and the average lead time of 304.68 days.

Table 11 shows the resulting regression model with only significant factors. As an example of using the regression model, consider the following factor values: a region with population of 650K, located in quadrant 1, an antiviral stockpile of 700K courses, antiviral treatment of visits to doctor, no NPI, a detection delay of 10 days, and $N = 6$. Based on the regression model, the outbreak lead time will be 35.94 days.

We also conducted ANOVA with Tukey tests to determine significant statistical difference in the factor levels. Table 12 summarizes which levels of each factor were found to be statistically different at the 0.05 level. Based on this table, a decision maker can conclude that for instance, blanket prophylaxis and contact tracing based treatment are expected to have similar effect on the outbreak lead time. On the other hand, the expected effect will be rather different for a 10-day and a 30-day detection delay as well as for the initial regions located in quadrants 1 and 3, respectively.

Table 13 shows the strategies that contained the outbreak at the source. Most of the strategies required the use of comprehensive NPI. It can also be observed that the blanket strategy was the most efficient of all antiviral distribution strategies. However, it did not prove to be statistically different than a combination of

Table 11: Regression Model for the Outbreak Lead Time

Factor	Coefficient	p-value
Intercept	-149.08	0.0001
P	0.0001178	0.0016
N	10.5057564	0.0003
AS	-0.0000669	< 0.0001
NPI	115.3587827	0.0017
D	8.7207832	< 0.0001
$Q \cdot AD$	35.9602963	< 0.0001
$Q \cdot NPI$	-120.3634501	< 0.0001
$Q \cdot D$	-2.2014098	0.0006
$P \cdot AD$	0.0000944	0.0019
$P \cdot NPI$	-0.0003678	< 0.0001
$P \cdot D$	-0.0000111	0.0001
$N \cdot AD$	8.2419937	< 0.0001
$N \cdot D$	-0.7762634	0.0002
$AS \cdot AD$	0.0001019	< 0.0001
$AS \cdot NPI$	0.0001491	< 0.0001
$AD \cdot NPI$	103.352587	< 0.0001
$AD \cdot D$	-3.5162046	< 0.0001
$NPI \cdot D$	-4.2564074	0.0003
$Q \cdot P \cdot AD$	-0.0000824	< 0.0001
$Q \cdot P \cdot NPI$	0.000318	< 0.0001
$Q \cdot P \cdot D$	0.0000048	0.0004
$P \cdot N \cdot AD$	-0.0000158	< 0.0001
$P \cdot N \cdot NPI$	0.0000167	< 0.0001
$P \cdot N \cdot D$	0.0000012	0.0003
$N \cdot AS \cdot NPI$	-0.0000045	0.0085
$N \cdot AS \cdot D$	0.0000003	< 0.0001
$AS \cdot AD \cdot NPI$	-0.0001031	< 0.0001
$AS \cdot AD \cdot D$	-0.0000017	< 0.0001
$AD \cdot NPI \cdot D$	4.8207876	< 0.0001

Q = region quadrant; P = population; N = number of infectious individuals required to start a regional outbreak; AS = antiviral stockpile; AD = antiviral distribution strategy; NPI = level of non-pharmaceutical interventions; D = detection delay.

Table 12: Factor Levels Grouped by Significance

Factor	Definition	Significant Levels
Q	Region quadrant	{1, 2}, {3}, {4}
P	Population (in thousands)	{195, 378}, {482}, {620, 646}, {931}
N	Number of infectious individuals required to start a regional outbreak	{3}, {6}, {10}
AS	Antiviral stockpile, courses	{0}, {260,000}, {2,000,000}
AD	Antiviral distribution strategy	{Treatment of visits to doctor}, {Contact tracing treatment, Blanket prophylaxis}
NPI	Level of non-pharmaceutical interventions	{None}, {Comprehensive}
D	Detection delay, days	{1}, {10}, {30}

contact tracing based treatment with comprehensive NPI. This result is important because the blanket distribution is expensive, very challenging logistically, and may increase the antiviral immunity of the virus. On the other hand, contact tracing based treatment implemented within 10 days of the pandemic detection and accompanied by comprehensive NPI appeared to have the same effect as the blanket policy but without any of the above disadvantages.

Table 13: Strategies Resulted in Outbreak Containment at the Source

	AS			AD			NPI		D		
Initial Outbreak	0	260K	2M	Treatment of doctor visits	Contact tracing treatment	Blanket Prophylaxis	0	1	1	10	30
All regions			*		*			*	*		
			*		*			*		*	
		*				*		*	*		
			*			*	*		*		
			*			*		*	*		
			*			*		*		*	
All regions but the largest (in addition to the above)		*			*			*	*		
			*		*			*			*
		*				*		*		*	
			*			*		*			*

The detection delay appeared to have a significant impact on the outbreak lead time. Outbreak containment at the source was possible for both a 1-day and a 10-day delay. This can suggest that a surveillance system does not have to be perfect to be effective. However, a 30-day delay led to a significant decrease in the lead time.

The number of infectious individuals required to start a regional outbreak, N, had a proportionate effect on the outbreak lead time. In our experience, setting this value too low may increase the noise in the simulation results, since some travelers may have limited social interaction in the destination regions. It appears that the effect of this variable on the lead time was approximately linear in the range between $N = 3$ and $N = 10$. However, this variable did not affect the set of strategies which led to outbreak containment at the source.

Appendix I shows a histogram of the lead time eliminating those simulations when an outbreak was contained at the source. The effect of all strategies in containing the outbreak at the source is presented in Appendix J.

7. Summary of Main Results, Contributions and Future Research

This dissertation presented three related models to aid decision makers to analyze resource sharing strategies during global influenza pandemics. The first model developed optimal capacity management strategies for a single lab to enhance multi-region pandemic surveillance. As it was shown in the later chapters, the detection delay could have a significant impact on the effectiveness of any resource sharing strategy. The second model estimated the outbreak lead time from the onset to a likely pandemic export region, such as a major transportation hub. The model served as the foundation for addressing the main objective of this dissertation. Substantial efforts were put to achieve accurate data support and computational feasibility of the model. The third model developed an empirical relationship to quantify the impact of various antiviral sharing strategies on the outbreak lead time under several pandemic detection and response scenarios.

7.1 Summary of the Main Results

Our study supports the claim that it is possible to contain an outbreak at the source. Table 13 lists different strategies to achieve this goal. In the majority of cases, the source containment was not possible without sharing of antivirals (2M courses). Both the blanket antiviral prophylaxis and the less costly contact tracing based treatment achieved at-source containment, but only when combined with a comprehensive NPI strategy and a prompt outbreak detection (within 10 days). Neither antiviral treatment of visits to doctor nor using only comprehensive NPI could achieve at-source containment.

In the worst case scenario, with no interventions, the 95% confidence interval for the mean outbreak lead time was $[43.2, 47.6]$ days. Using only comprehensive NPI

without antivirals yielded the confidence interval of $[163.8, 207.2]$ days with at-source containment achieved in only 5% of the time. In the most optimistic scenario of implementing both comprehensive non-pharmaceutical interventions and blanket/contact tracing based antiviral strategies (with 2M courses), with a prompt detection (within 10 days), the corresponding confidence interval was $[580.6, 600.0]$ days with at-source containment achieved in 98% of the time.

The impact of the factors on the outbreak lead time was nonlinear and complex with some factors and interactions being more influential than others. All of the factors considered in the design of experiment were found to be significant, either by themselves or through factor interactions. In all cases, outbreak containment was achieved at the source while none was achieved in transit to a LPE region.

Mexico and Guadalajara were the most recurrent LPE regions with approximately 80% of all pandemic paths ending in these two major cities. It can be suggested that these regions need special PI surveillance once an outbreak is detected, particularly at the airports and bus stations. From the standpoint of Mexico partners, it can also be suggested that restricting incoming travel from the above regions may be a more appealing option than banning the air traffic from the entire country. It was found that touristic LPE regions were among the least affected LPE regions unless an outbreak started in a nearby area. Not all regions of the country were equally affected by pandemic. The areas on the intersection of major highways were among the most affected and thus requiring higher surveillance, whereas the areas with low population density (such as deserts in the northern part of the country) seemed to be less impacted and hence needing less surveillance.

The propagation of a PI outbreak was highly correlated with the transportation network and the regional demographics. It was observed in some isolated cases that small and less connected regions could contain the outbreak without interventions. While eventually the virus may escape such small isolated regions, with adequate

surveillance, public health officials would be able to develop a potent vaccine to protect the rest of the country population.

To enhance the U.S. preparedness and response, it is necessary to assist the developing countries to establish adequate surveillance systems. We have shown that these systems do not have to be perfect to be effective, and that sampling of specimens should be distributed differently among the regions. For surveillance to be effective, it needs to focus on economically undeveloped areas, regions with high connectivity, and likely pandemic export regions.

7.2 Main Contributions

Our work is one of the first decision models for a quantitative assessment of resource sharing strategies during global pandemic scenarios. We have developed an empirical relationship for the outbreak lead time. Our results demonstrate the importance of considering both the regional heterogeneity and comprehensive travel networks in pandemic models. Our research is also an initial attempt to develop a detailed simulation of pandemic spread and mitigation strategies in Mexico. Such a study is important because of the precedence of H1N1/2009, a virus with high transmissibility and low severity, that demonstrated the inadequacy of the existing international collaboration. Mexico also stands as the U.S. nearest possible pandemic incubator. We hope that the above contributions will help to enhance the U.S. preparedness and response planning for influenza pandemics.

7.3 Future Research

The outbreak detection delay was found to be a significant determinant of the effectiveness of any resource sharing strategy. The ability of our model to project expected outbreak paths can pinpoint the regions requiring higher level of surveillance. Hence, one of the future research opportunities would be to support the design of an efficient countrywide surveillance system, including the number and placement of

laboratories and development of sampling strategies. In particular, we would like to explore the logistics required for a Mexican pandemic surveillance system.

Our conclusions were drawn based on a testbed of Mexico. At this point, we cannot say whether the conclusions will apply to other countries, particularly those with different regional demographics and the prevalent domestic transportation modes. Moreover, we have only considered a "one country - one country" type of collaboration. It will be both desirable and very challenging to examine international collaboration involving multiple resource donors and pandemic incubators. A necessary part of such examination will be the design of an improved global outbreak alert and response network (GOARN).

References

[1] M. E. Halloran, N. M. Ferguson, S. Eubank, and I. Longini, "Modeling targeted layered containment of an influenza pandemic in the United States," *PNAS*, vol. 105, no. 12, pp. 4639–4644, 2008.

[2] P. D. Ellner and H. C. Neu, *Understanding Infectious Disease*. Mosby Year Book, 1992.

[3] P. Davies, *The Devil's Flu*. Henry Holt and Company, first ed., 2000.

[4] World Health Organization (WHO), "H5N1 avian influenza:Timeline of major events." http://www.who.int/csr/disease/avian_influenza/Timeline090727.pdf. Last accessed on 08/28/2009.

[5] World Health Organization (WHO), "Cumulative number of confirmed human cases of Avian Influenza A/(H5N1) reported to WHO." http://www.who.int/csr/disease/avian_influenza/country/cases_table_2008_08_11/en/index.html. Last accessed on 08/28/2009.

[6] World Health Organization (WHO), "Influenza-like illness in the United States and Mexico." http://www.who.int/csr/don/2009_04_24/en/index.html. Last accessed on 08/28/2009.

[7] World Health Organization (WHO), "Pandemic (H1N1) 2009 – update 62." http://www.who.int/csr/don/2009_08_21/en/index.html. Last accessed on 08/28/2009.

[8] World Health Organization (WHO), "Pandemic (H1N1) 2009 – update 70." http://www.who.int/csr/don/2009_10_16/en/index.html, October 2009. Last accessed on 11/06/2009.

[9] L. Garrett, *"The coming plague: newly emerging diseases in a world without balance"*. Penguin Books, first ed., 1995.

[10] N. M. Ferguson, D. Cummings, S. Cauchemez, C. Fraser, S. Riley, M. Aronrag, S. Lamsirithaworn, and D. Burke, "Strategies for containing an emerging influenza pandemic in southeast asia," *Nature*, vol. 437, pp. 209–214, 2005.

[11] A. Sidorenko, "Global macroeconomic consequences of pandemic influenza," tech. rep., Lowy Institute for International Policy, 31 Bligh Street Sidney NSW 2000 Australia, February 2006.

[12] Centers for Disease Control and Prevention (CDC), "Interim Guidance for the Detection of Novel Influenza A Virus Using Rapid Influenza Diagnostic Tests." http://www.cdc.gov/h1n1flu/guidance/rapid_testing.htm, 2009. Last accessed on 11/06/2009.

[13] S. Mniszewski, S. del Valle, P. Stroud, J. Riese, and S. Sydoriak, "Pandemic simulation of antivirals + school closures: buying time until strain-specific vaccine is available," *Comput. Math Organ. Theory*, no. 14, pp. 209–221, 2008.

[14] The New York Times, "Swine flu (H1N1) vaccine." http://www.nytimes.com/info/swine-flu-h1n1-vaccine/. Last accesed on 11/06/2009.

[15] U.S. Department of Health & Human Services, "HHS pandemic influenza plan." http://www.hhs.gov/pandemicflu/plan/, 2007. Last accessed on 03/27/2009.

[16] I. M. Longini, A. Nizam, X. Shufu, K. Ungchusak, W. Hanshaoworakul, D. Cummings, and M. E. Halloran, "Containing pandemic influenza at the source," *Science*, vol. 309, pp. 1083–1087, 2005.

[17] H. Oshitani, T. Kamigaki, and A. Suzuki, "Major issues and challenges of influenza pandemic preparedness in developing countries," *Emerging infectious diseases*, vol. 14, no. 6, p. 875, 2008.

[18] F. Carrat, A. Lavenu, S. Cauchemez, and S. Deleguer, "Repeated influenza vaccination of healthy children and adults: borrow now, pay later?," *Epidemiol. Infect.*, vol. 134, p. 6370, 2005.

[19] N. Becker and D. Starczak, "Optimal vaccination strategies for a community of households," *Mathematical Biosciences*, vol. 139, pp. 117–132, 1997.

[20] I. M. Longini and J. S. Koopman, "Household and community transmission parameters from final distributions of infections in households.," *Biometrics*, vol. 38, no. 115-126, 1982.

[21] Y. Tang, I. Longini, and M. Halloran, "Design and evaluation of prophylactic interventions using disease incidence data from close contact groups," *Applied Statistics*, vol. 55, no. 3, pp. 317–330, 2006.

[22] S. Cauchemez, F. Carrat, C. Viboud, A. Valleron, and P. Boelle, "A bayesian mcmc approach to study transmission of influenza: application to household longitudinal data," *Statist. Med.*, vol. 23, p. 34693487, 2004.

[23] F. Ball and O. Lyne, "Optimal vaccination policies for stochastic epdidemics among a population of households," *Mathematical Biosciences*, vol. 177-178, pp. 333–354, 2002.

[24] R. Larson, "Simple models of influenza progression within a heterogeneous population," *Operations Research*, vol. 55, no. 399-412, pp. 165–195, 2007.

[25] J. Arino, F. Brauer, P.van den Driessche, J. Watmough, and J. Wu, "Simple models for containment of a pandemic," *J. R. Soc. Interface*, vol. 3, pp. 453–457, 2006.

[26] M. Atkinson and L. Wein, "Quantifying the routes of transmission for pandemic influenza," *Bulletin of Mathematical Biology*, no. 70, pp. 820–867, 2008.

[27] J. Mathews, C. McCaw, J. McVernon, E. McBride, and J. McCaw, "A biological model for influenza transmission: Pandemic planning implications of asymptomatic infection and immunity," *Plos One*, vol. 2, pp. 1–6, November 2007.

[28] N. Ferguson, D. A. Cummings, C. Fraser, J. Cajka, P. C. C., and D. S. Burke, "Strategies for mitigating an influenza pandemic," *Nature*, vol. 442, no. 27, pp. 448–452, 2006.

[29] T. Germann, K. Kadau, I. M. Longini, and C. Macken, "Mitigation strategies for pandemic influenza in the United States," *PNAS*, vol. 103, pp. 5935–5940, 2006.

[30] S. Eubank, "Network based models of infectious disease spread," *Japanese J Infec Dis*, vol. 58, pp. S9–S13, 2005.

[31] Oak Ridge National Laboratory, "Landscan global population data." http://www.ornl.gov/sci/landscan, 2007.

[32] R. J. Glass, L. M. Glass, W. E. Beyeler, and H. J. Min, "Targeted social distancing design for pandemic influenza," *Emerg. Infec. Dis.*, vol. 12, no. 11, pp. 1671–1681, 2006.

[33] J. T. Wu, S. Riley, C. Fraser, and G. Leung, "Reducing the impact of the next influenza pandemic using household-based public health interventions," *PLoS Med*, vol. 3, no. 9, pp. 1532–1540, 2006.

[34] P. Cooley, L. Ganapathi, G. Ghneim, S. Holmberg, W. Wheaton, and C. Hollingsworth, "Using influenza-like illness data to reconstruct an influenza outbreak," *Mathematical and Computer Modelling*, no. 48, pp. 929–939, 2008.

[35] T. Das, A. Savachkin, and Y. Zhu, "A large scale simulation model of pandemic influenza outbreaks for assessment of societal risk and development of dynamic mitigation strategies," *IIE Transactions*, vol. 40, no. 9, pp. 893–905, 2008.

[36] A. Uribe, A. Savachkin, T. Das, A. Santana, and D. Prieto, "A predictive decision aid methodology for dynamic mitigation of influenza pandemics," *accepted for publication in OR Spectrum*, 2011.

[37] Eclipse, Foundation, "The Spatio-Temporal Epidemiological Modeler." http://www.eclipse.org/stem/intro.php, 2009. Last accessed on 11/06/2009.

[38] V. Colizza, A. Barrat, M. Barthelemy, and A. Vespignani, "The role of the airline transportation network in the prediction and predictability of global epidemics," *PNAS*, vol. 103, pp. 2015–2020, 2006.

[39] V. Colizza, A. Barrat, M. Barthelemy, A. Valleron, and A. Vespignani, "Modeling the worldwide spread of pandemic influenza: Baseline case and containment interventions," *PLoS Medicine*, vol. 4, no. 1, p. 95, 2007.

[40] T. Das, and A. Savachkin, "A large scale simulation model for assessment of societal risk and development of dynamic mitigation strategies," *IIE Transactions*, vol. 99, no. 9, p. 129, 2008.

[41] A. Savachkin, T. Das, D. Prieto, and A. Uribe, "A bi-level stochastic optimization model for pandemic mitigation," *Working Paper*, 2009.

[42] R. Guimera, S. Mossa, A. Turtschi, and L. Amaral, "The worldwide air transportation network: Anomalous centrality, community structure, and cities' global roles," *Proceedings of the National Academy of Sciences of the United States of America*, vol. 102, no. 22, p. 7794, 2005.

[43] G. Bobashev, R. Morris, and D. Goedecke, "Sampling for Global Epidemic Models and the Topology of an International Airport Network," *PLoS One*, vol. 3, no. 9, 2008.

[44] M. Patel, C. Phillips, C. Pearce, M. Kljakovic, P. Dugdale, and N. Glasgow, "General practice and pandemic influenza: a framework for planning and comparison of plans in five countries," *PLoS One*, vol. 3, no. 5, p. 2269, 2008.

[45] P. Hanvoravongchai, W. Adisasmito, P. Chau, A. Conseil, J. De Sa, R. Krumkamp, S. Mounier-Jack, B. Phommasack, W. Putthasri, C. Shih, *et al.*, "Pandemic influenza preparedness and health systems challenges in Asia: results from rapid analyses in 6 Asian countries," *BMC Public Health*, vol. 10, no. 1, p. 322, 2010.

[46] A. Mensua, S. Mounier-Jack, and R. Coker, "Pandemic influenza preparedness in Latin America: analysis of national strategic plans," *Health Policy and Planning*, 2009.

[47] "North american plan for avian and pandemic influenza," tech. rep., Security and Prosperity Partnership of North America, August 2007.

[48] C. McDougall, R. Upshur, and K. Wilson, "Emerging norms for the control of emerging epidemics," *Bulletin of the World Health Organization*, vol. 86, pp. 643–645, 2008.

[49] K. Paranthaman, C. Conlon, C. Parker, and N. McCarthy, "Resource allocation during an influenza pandemic," *Emerging Infectious Diseases*, vol. 14, no. 3, p. 520, 2008.

[50] A. Thompson, K. Faith, J. Gibson, and R. Upshur, "Pandemic influenza preparedness: an ethical framework to guide decision-making," *BMC Medical Ethics*, vol. 7, no. 1, p. 12, 2006.

[51] C. Franco-Paredes, P. Carrasco, and J. Preciado, "The first influenza pandemic in the new millennium: lessons learned hitherto for current control efforts and overall pandemic preparedness," *Journal of Immune Based Therapies and Vaccines*, vol. 7, no. 1, p. 2, 2009.

[52] W. Gallaher, "Towards a sane and rational approach to management of Influenza H 1 N 1 2009," *Virology journal*, vol. 6, no. 1, p. 51, 2009.

[53] R. Katz, "Use of revised international health regulations during influenza A (H1N1) epidemic, 2009," *Emerging Infectious Diseases*, vol. 15, no. 8, p. 1165, 2009.

[54] C. Fraser, C. Donnelly, S. Cauchemez, W. Hanage, M. Van Kerkhove, T. Hollingsworth, J. Griffin, R. Baggaley, H. Jenkins, E. Lyons, *et al.*, "Pandemic potential of a strain of influenza A (H1N1): early findings," *Science*, vol. 324, no. 5934, p. 1557, 2009.

[55] B. Coburn, B. Wagner, and S. Blower, "Modeling influenza epidemics and pandemics: insights into the future of swine flu(H 1 N 1)," *BMC medicine*, vol. 7, no. 1, p. 30, 2009.

[56] N. Aburto, E. Pevzner, R. Lopez-Ridaura, R. Rojas, H. Lopez-Gatell, E. Lazcano, M. Hernandez-Avila, and T. Harrington, "Knowledge and Adoption of Community Mitigation Efforts in Mexico During the 2009 H1N1 Pandemic," *American journal of preventive medicine*, vol. 39, no. 5, pp. 395–402, 2010.

[57] S. Echevarría-Zuno, J. Mejía-Aranguré, A. Mar-Obeso, C. Grajales-Muñiz, E. Robles-Pérez, M. González-León, M. Ortega-Alvarez, C. Gonzalez-Bonilla, R. Rascón-Pacheco, and V. Borja-Aburto, "Infection and death from influenza A H1N1 virus in Mexico: a retrospective analysis," *The Lancet*, vol. 374, no. 9707, pp. 2072–2079, 2010.

[58] N. Halder, J. Kelso, and G. Milne, "Analysis of the effectiveness of interventions used during the 2009 A/H 1 N 1 influenza pandemic," *BMC Public Health*, vol. 10, no. 1, p. 168, 2010.

[59] F. Loustalot, B. Silk, A. Gaither, T. Shim, M. Lamias, F. Dawood, O. Morgan, D. Fishbein, S. Guerra, J. Verani, *et al.*, "Household Transmission of 2009 Pandemic Influenza A (H1N1) and Nonpharmaceutical Interventions among Households of High School Students in San Antonio, Texas," *Clinical Infectious Diseases*, vol. 52, no. suppl 1, p. S146, 2011.

[60] A. Stern and H. Markel, "What Mexico taught the world about pandemic influenza preparedness and community mitigation strategies," *JAMA*, vol. 302, no. 11, p. 1221, 2009.

[61] V. Colizza, A. Vespignani, N. Perra, C. Poletto, B. Gonçalves, H. Hu, D. Balcan, D. Paolotti, W. Van den Broeck, M. Tizzoni, *et al.*, "Estimate of Novel Influenza A/H1N1 cases in Mexico at the early stage of the pandemic with a spatially structured epidemic model,"

[62] M. Lipsitch, M. Lajous, J. O'Hagan, T. Cohen, J. Miller, E. Goldstein, L. Danon, J. Wallinga, S. Riley, S. Dowell, *et al.*, "Use of cumulative incidence of novel influenza a/h1n1 in foreign travelers to estimate lower bounds on cumulative incidence in mexico," *PLoS one*, vol. 4, no. 9, p. e6895, 2009.

[63] Committee on Modeling Community Containment for Pandemic Influenza, "Modeling community containment for pandemic influenza: A letter report." http://www.nap.edu/catalog/11800.html, 2006.

[64] C. Reed, F. Angulo, D. Swerdlow, M. Lipsitch, M. Meltzer, D. Jernigan, and L. Finelli, "Estimates of the prevalence of pandemic (H1N1) 2009, United States, April–July 2009," *Emerging Infectious Diseases*, vol. 15, no. 12, pp. 2004–7, 2009.

[65] INEGI, "Annual statistics report by state 2010," tech. rep., National Institute of Statistics, Geography and Informatics, Mexico, 2010.

[66] INEGI, "Sistema automatizado de información censal saic 5.0," tech. rep., National Institute of Statistics, Geography and Informatics, Mexico, 2007.

[67] Mexican Institute of Transportation, "Manual estadístico del sector transporte 2009," tech. rep., 2009.

[68] INEGI, "Sistema para la consulta de indicadores estratégicos infolaboral." http://www.inegi.org.mx/est/contenidos/espanol/sistemas/enoe/infoenoe/ default.aspx, 2011. Last accessed 02/20/2011.

[69] INEGI, "Derehohabiencia y uso de servicios de salud." http://www.inegi.org.mx/sistemas/sisept/default.aspx, 2011. Last accessed 02/20/2011.

[70] Secretary of Communications and Transportation, "Basics statistics of federal transportation," tech. rep., SCT, Mexico, 2009.

[71] INEGI, "Marco geoestadístico municipal 2005," tech. rep., National Institute of Statistics, Geography and Informatics, Mexico, 2005.

[72] Autobuses Estrella Blanca, "Customer service website." http://www.estrellablanca.com.mx/, 2010. Last accessed on 11/10/2010.

[73] Omnibus de Mexico, "Customer service website." http://www.odm.com.mx/, 2010. Last accessed on 11/10/2010.

[74] Autotransportes Baja California, "Customer service website." http://www.abc.com.mx/home.aspx, 2010. Last accessed on 11/10/2010.

[75] A. Uribe-Sánchez and A. Savachkin, "Two resource distribution strategies for dynamic mitigation of influenza pandemics," *Journal of Multidisciplinary Healthcare*, vol. 3, pp. 65–77, 2010.

Appendices

Appendix A

Repository of Mexico Data

In this appendix we list all regions, their population, quadrant classification, and coordinates, shown in Figure 13. The national average percentage of industrial businesses was 35% while the national mean of the average business size was 4.8 employees.

Appendix A (Continued)

Table A1: Repository of Mexico Data

Region	Quadrant	Population	% of Industrial Businesses	Average Company Size
1. Pinos, Zacatecas	1	825,881	32.5%	2.5
2. Fresnillo, Zacatecas	1	551,896	33.9%	4.2
3. Tizimín, Yucatán	2	1,043,294	42.8%	3.5
4. Mérida, Yucatán	3	781,549	38.7%	6.4
5. Tierra Blanca, Veracruz	2	883,261	37.3%	2.8
6. Martínez de la Torre, Veracruz	2	680,586	36.0%	2.8
7. Tantoyuca, Veracruz	2	622,439	37.1%	3.0
8. Poza Rica de Hidalgo, Veracruz	1	1,025,364	34.7%	3.4
9. Coatepec, Veracruz	1	1,184,980	32.2%	2.9
10. Veracruz, Veracruz	3	654,410	38.0%	6.5
11. San Andrés Tuxtla, Veracruz	1	303,827	35.1%	3.1
12. Córdoba, Veracruz	2	520,710	36.1%	4.4
13. Coatzacoalcos, Veracruz	2	877,007	35.5%	4.5
14. Xalapa, Enríquez, Veracruz	2	482,113	40.8%	4.1
15. Tlaxcala de Xicohténcatl, Tlaxcala	2	583,922	37.1%	3.2
16. Huamantla, Tlaxcala	1	503,078	32.5%	3.3
17. San Fernando, Tamaulipas	1	206,541	33.7%	3.3
18. Heroica Matamoros, Tamaulipas	3	527,595	40.6%	8.2
19. Ciudad Victoria, Tamaulipas	2	589,529	37.9%	4.7

Appendix A (Continued)

Table A1 (Continued)

Region	Quadrant	Population	% of Industrial Businesses	Average Company Size
20. Tampico, Tamaulipas	3	661,272	39.7%	6.5
21. Reynosa, Tamaulipas	3	636,551	36.5%	9.3
22. Nuevo Laredo, Tamaulipas	3	423,964	40.4%	5.8
23. Macuspana, Tabasco	2	526,887	39.1%	3.3
24. Cunduacán, Tabasco	2	349,645	43.4%	3.6
25. Cárdenas, Tabasco	2	557,294	36.3%	4.0
26. Villahermosa, Tabasco	3	558,569	40.1%	6.3
27. Ciudad Obregón, Sonora	3	600,291	44.3%	6.3
28. Navojoa, Sonora	2	432,274	40.5%	4.6
29. Heroica Nogales, Sonora	3	679,908	40.8%	7.2
30. Hermosillo, Sonora	3	704,542	47.0%	7.3
31. Navolato, Sinaloa	2	469,209	37.4%	4.2
32. Mazatlán, Sinaloa	3	620,821	40.7%	6.0
33. Guasave, Sinaloa	3	738,985	42.5%	5.2
34. Culiacán Rosales, Sinaloa	3	796,335	44.6%	6.1
35. Rioverde, San Luis Potosí	1	819,897	28.3%	3.1
36. Ciudad Valles, San Luis Potosí	2	646,287	36.8%	3.2
37. San Luis Potosí, San Luis Potosí	3	959,906	39.5%	6.3
38. Cozumel, Quintana Roo	4	728,854	31.3%	6.1

Appendix A (Continued)

Table A1 (Continued)

Region	Quadrant	Population	% of Industrial Businesses	Average Company Size
39. Cancún, Quintana Roo	3	574,441	36.0%	8.7
40. Cadereyta de Montes, Querétaro	1	237,688	26.9%	3.1
41. San Juan del Río, Querétaro	3	630,763	37.5%	6.4
42. Santiago de Querétaro, Querétaro	3	734,608	36.6%	6.7
43. Tehuacan, Puebla	2	553,986	39.2%	4.3
44. Huauchinango, Puebla	1	676,386	35.0%	2.4
45. Teziutlan, Puebla	2	432,106	37.3%	3.9
46. Atlixco, Puebla	1	504,321	34.4%	2.5
47. Amozoc de Mota, Puebla	1	524,514	34.1%	2.6
48. Heroica Puebla de Zaragoza, Puebla	3	1,486,068	36.3%	5.1
49. Palmar de Bravo, Puebla	2	805,462	39.0%	2.2
50. San Martin Texmelucan de	2	500,730	39.3%	4.8
51. Santiago Pinotepa Nacional, Oaxaca	1	1,037,783	32.1%	2.4
52. San Juan Bautista Valle Nacional, Oaxaca	2	424,182	38.4%	2.8
53. Heroica Ciudad de Huajuapan de León,	1	398,818	28.6%	2.6
54. Santo Domingo Tehuantepec, Oaxaca	1	613,411	32.2%	2.9
55. Oaxaca de Juárez, Oaxaca	1	456,488	33.2%	3.6
56. Salina Cruz, Oaxaca	2	352,193	40.6%	2.8
57. San Juan Bautista Tuxtepec, Oaxaca	2	477,403	37.6%	3.2

Appendix A (Continued)

Table A1 (Continued)

Region	Quadrant	Population	% of Industrial Businesses	Average Company Size
58. Ciudad San Nicolás de los Garza, Nuevo	3	476,761	39.1%	10.1
59. Ciudad Monterrey, Nuevo León	3	1,133,826	41.5%	9.0
60. Ciudad Benito Juárez, Nuevo León	4	249,559	33.7%	6.0
61. Ciudad Guadalupe, Nuevo León	3	691,965	37.7%	6.4
62. Ciudad General Escobedo, Nuevo León	4	299,428	27.2%	6.5
63. Ciudad Santa Catarina, Nuevo León	3	382,039	42.2%	15.7
64. Ciudad Apodaca, Nuevo León	4	418,971	32.5%	14.5
65. Linares, Nuevo León	4	560,331	33.4%	6.0
66. Tepic, Nayarit	2	678,365	38.0%	4.0
67. Acaponeta, Nayarit	1	279,019	34.2%	3.5
68. Yautepec de Zaragoza, Morelos	1	759,546	29.7%	2.7
69. Cuernavaca, Morelos	1	698,204	34.5%	4.4
70. Cuautla, Morelos	1	160,339	29.9%	2.9
71. Puruándiro, Michoacán	1	931,317	32.5%	2.7
72. Heroica Zitácuaro, Michoacán	2	550,109	35.6%	2.5
73. Uruapan, Michoacán	2	916,206	41.4%	3.2
74. La Piedad de Cabadas, Michoacán	2	348,460	35.7%	3.1
75. Pátzcuaro, Michoacán	2	214,324	46.7%	2.5
76. Apatzingán de la Constitución, Michoacán	2	179,115	35.3%	2.8

Appendix A (Continued)

Table A1 (Continued)

Region	Quadrant	Population	% of Industrial Businesses	Average Company Size
77. Morelia, Michoacán	2	684,373	39.0%	4.2
78. Ciudad Lázaro Cárdenas, Michoacán	1	163,367	34.3%	4.4
79. Ciudad de México, Distrito Federal	4	19,308,938	33.1%	6.4
80. Ixtlahuaca de Rayón, México	1	1,472,902	29.8%	4.3
81. Toluca de Lerdo, México	4	747,536	33.0%	5.5
82. Amecameca de Juárez, México	1	213,118	29.1%	2.5
83. Texcoco de Mora, México	1	490,663	32.7%	3.0
84. Metepec, México	1	282,906	31.5%	3.8
85. Tenancingo de Degollado, México	1	1,590,998	28.9%	3.4
86. Autlán de Navarro, Jalisco	1	589,289	31.5%	3.0
87. Ciudad Guzmán, Jalisco	2	195,554	36.4%	3.2
88. Zapopan, Jalisco	3	1,156,203	37.4%	8.1
89. Ocotlán, Jalisco	4	761,727	32.6%	6.0
90. Lagos de Moreno, Jalisco	1	910,743	33.1%	3.7
91. Tequila, Jalisco	1	111,663	25.9%	3.2
92. Tonalá, Jalisco	2	408,805	36.5%	3.2
93. Tlaquepaque, Jalisco	4	563,086	34.4%	4.9
94. Tala, Jalisco	1	261,837	31.4%	3.1
95. Puerto Vallarta, Jalisco	4	220,558	32.7%	6.2

Appendix A (Continued)

Table A1 (Continued)

Region	Quadrant	Population	% of Industrial Businesses	Average Company Size
96. Guadalajara, Jalisco	3	1,600,954	39.8%	6.7
97. Tula de Allende, Hidalgo	1	775,896	34.5%	4.2
98. Pachuca de Soto, Hidalgo	2	660,334	36.7%	4.2
99. Tulancingo, Hidalgo	2	391,654	37.1%	3.1
100. Huejutla de Reyes, Hidalgo	1	530,640	33.4%	2.8
101. Chilpancingo de los Bravo, Guerrero	1	391,281	31.6%	2.6
102. Teloloapan, Guerrero	2	312,102	51.2%	2.4
103. Ixtapa Zihuatanejo, Guerrero	1	648,020	31.1%	3.1
104. Iguala de la Independencia,	2	251,638	39.1%	2.5
105. Tlapa de Comonfort, Guerrero	1	774,876	31.3%	2.2
106. Acapulco de Juárez, Guerrero	1	718,103	28.8%	4.6
107. Acámbaro, Guanajuato	1	638,594	31.3%	2.7
108. Guanajuato, Guanajuato	1	799,418	31.3%	4.3
109. San Miguel de Allende, Guanajuato	1	486,713	30.8%	4.0
110. Irapuato, Guanajuato	2	698,654	35.4%	4.7
111. Pénjamo, Guanajuato	2	592,141	35.4%	3.9
112. León de los Aldama, Guanajuato	3	1,279,590	39.1%	6.3
113. Celaya, Guanajuato	3	416,539	37.7%	5.3
114. El Salto, Durango	1	563,483	29.6%	3.5

Appendix A (Continued)

Table A1 (Continued)

Region	Quadrant	Population	% of Industrial Businesses	Average Company Size
115. Gómez Palacio, Durango	3	435,114	37.3%	9.4
116. Victoria de Durango, Durango	3	528,557	42.5%	4.9
117. Guadalupe y Calvo, Chihuahua	1	423,728	31.9%	4.0
118. Delicias, Chihuahua	3	225,008	35.6%	5.3
119. Hidalgo del Parral, Chihuahua	2	119,061	36.5%	4.5
120. Cuauhtémoc, Chihuahua	3	436,736	35.8%	7.6
121. Juárez, Chihuahua	3	1,314,400	35.5%	11.8
122. Chihuahua, Chihuahua	3	759,493	39.2%	8.9
123. Tila, Chiapas	1	446,808	17.4%	2.4
124. Ocosingo, Chiapas	1	613,709	21.1%	2.6
125. Chiapa de Corzo, Chiapas	1	212,892	28.1%	2.8
126. Venustiano Carranza, Chiapas	1	492,055	29.3%	2.5
127. Villaflores, Chiapas	1	519,985	34.1%	3.0
128. Tapachula de Córdova y Ordóñez,	1	635,905	32.0%	3.1
129. Tuxtla Gutiérrez, Chiapas	2	568,792	35.5%	4.2
130. La Trinitaria, Chiapas	1	195,868	22.7%	2.3
131. Reforma, Chiapas	1	311,157	24.7%	4.1
132. San Cristóbal de las Casas, Chiapas	1	333,800	27.5%	3.0
133. Comitán de Domínguez, Chiapas	1	184,008	29.5%	2.3

Appendix A (Continued)

Table A1 (Continued)

Region	Quadrant	Population	% of Industrial Businesses	Average Company Size
134. Colima, Colima	2	237,878	41.3%	4.7
135. Manzanillo, Colima	1	263,524	34.6%	4.5
136. Cuauhtémoc, Colima	1	70,684	29.1%	3.4
137. Ciudad Acuña, Coahuila	4	212,788	30.3%	13.3
138. San Buenaventura, Coahuila	4	56,358	28.1%	6.3
139. Parras de la Fuente, Coahuila	4	90,242	27.0%	5.5
140. Torreón, Coahuila	3	1,155,364	40.5%	8.6
141. Matamoros, Coahuila	1	246,271	30.2%	4.3
142. Piedras Negras, Coahuila	3	292,553	35.6%	8.4
143. Saltillo, Coahuila	3	727,500	37.3%	8.0
144. Monclova, Coahuila	4	303,368	35.2%	7.2
145. Ciudad del Carmen, Campeche	4	378,869	35.1%	6.7
146. Hopelchén, Campeche	1	58,972	23.3%	3.1
147. Campeche, Campeche	2	326,394	36.4%	4.5
148. Santa Rosalía, Baja California Sur	2	133,106	43.7%	4.3
149. La Paz, Baja California Sur	3	387,716	41.9%	5.8
150. Tijuana, Baja California	3	1,485,310	40.6%	9.8
151. Ensenada, Baja California	3	510,367	41.3%	6.3
152. Mexicali, Baja California	3	860,288	43.0%	8.9

Appendix A (Continued)

Table A1 (Continued)

Region	Quadrant	Population	% of Industrial Businesses	Average Company Size
153. Aguascalientes, Aguascalientes	3	877,498	38.1%	6.2
154. Rincón de Romos, Aguascalientes	1	136,762	27.3%	3.8
155. Calvillo, Aguascalientes	1	58,180	30.6%	3.2

Appendix B

Simulator Flow Graph

The following figure represents a flowchart of the single-region simulation model.

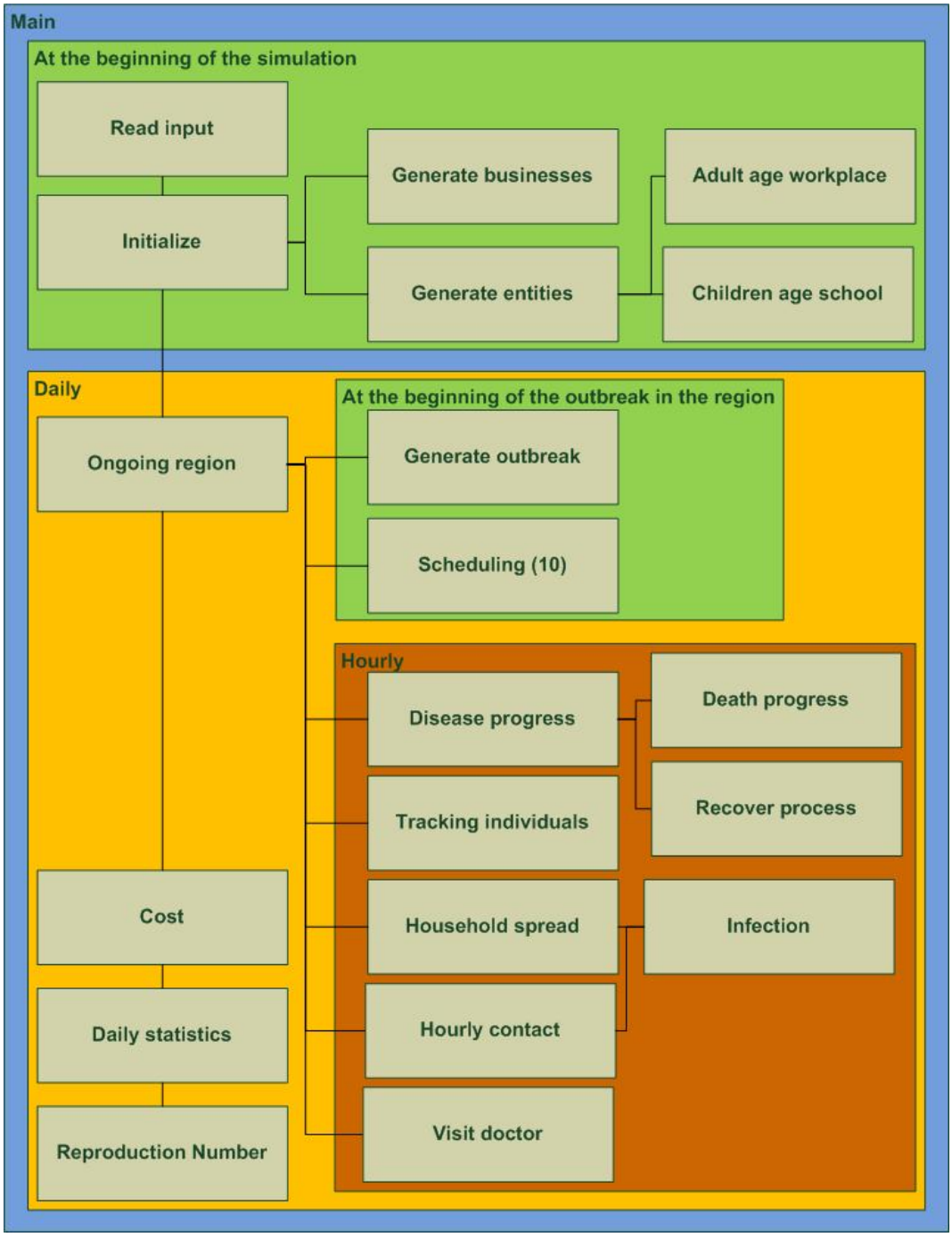

Figure B1: Simulator Flow Graph

Appendix C

Input and Output Files

Table C1: Input Files

File name	Content
age_children.txt	Column 1: Age group Column i+1: CDF of region i, for i=1,2,...,155 Column 157: School type Column 158: Age group
age_adults.txt	Column 1: Age group Column i+1: CDF of region i, for i=1,2,...,155 Column 157: Age group
households.txt	Column 1: Number of adults in the household Column 2: Number of children in the household Column i+2: CDF of region i, for i=1,2,...,155
workplaces.txt	Column 1: Business type Column 2i: Number of businesses per type in region i, for i=1,2,...,155 Column 2i+1: CDF of people working in each businesses type in region i, for i=1,2,...,155 Column 312: Number of subgroups Column 313: Percentage of weekday errands Column 314: Percentage of weekend errands Column 315: Percentage of voluntary quarantine errands
travel.txt	Column 1 and Row 1: Region ID Column i, Row j: Probability to travel from Region i to Region j, for i=1,2,...,155, and j=1,2,...,155
serologic.txt	Column 1: Lower bound age Column 2: Upper bound age Column 3: Scale factor
mortality.txt	Column 1: Age group Column 2: Mortality probability
contact_probability.txt	Column 1: Contact type Columns 2 and 3: Not used Column 4: Contact probability

Appendix C (Continued)

Table C2: Output Files

File name	Content
SummaryRegion.txt	Region ID Day Population size Number of workplaces Number of mixing groups Antiviral risk group Vaccination risk group Region status Total cost Dead cost Quarantine cost Daily contacts Daily infected cases Daily fatality ratio Infected Infected by age group Recovered Recovered by age group Deaths Deaths by age group Asymptomatic cases Visits to doctor Visits to doctor by age group Individuals in quarantine Individuals in quarantine by age group Antiviral stockpile Vaccination capacity Vaccine stockpile Vaccination period Quarantine compliance Quarantine category
ContactProcess.txt	Day Daily contacts Daily infected cases Daily contacts in households and workplaces Daily infected cases in households and workplaces
ReproductionNumber.txt	Region ID Day Daily infection number Sum reproduction number Average reproduction number

Appendix D

Relationships in the Scenario Manager

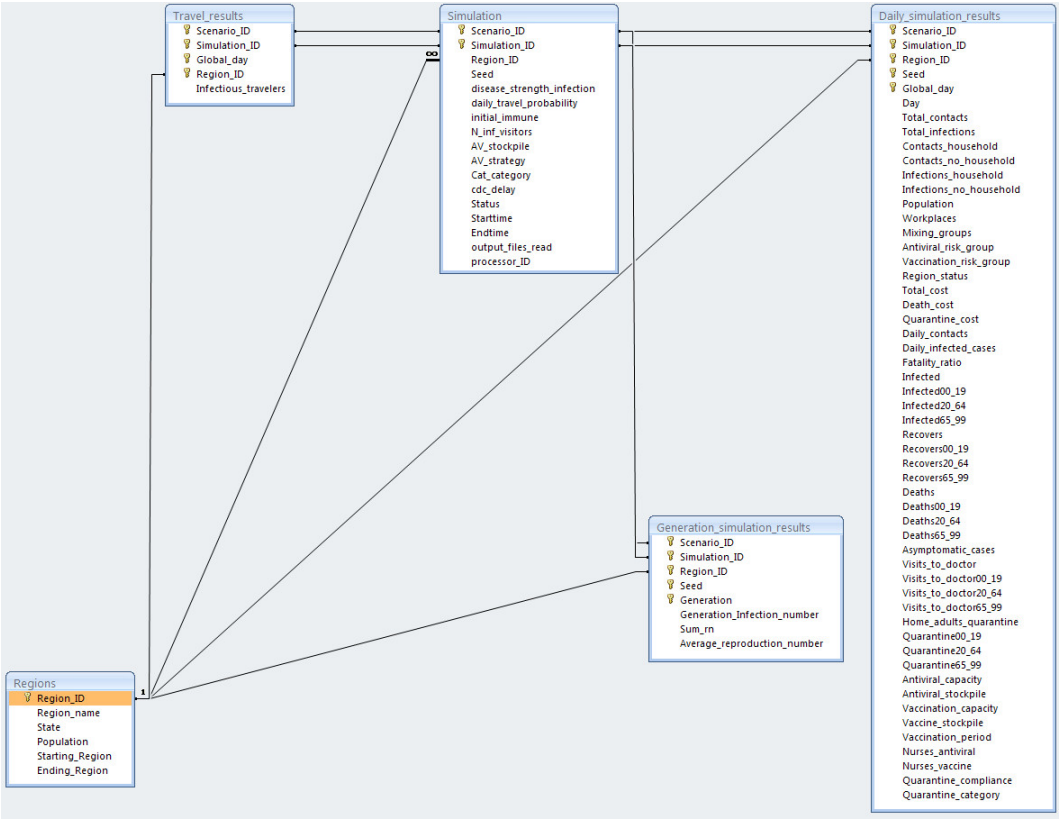

Figure D1: Relationships in the Scenario Manager

Appendix E

Calibration Values

In this appendix, we summarize the values obtained from the calibration process. We display the values of $\rho = 1100, 1175, 1250, 1325, 1575$ since they were the most common stable values obtained for most of the regions and seeds. However, some regions had their stable values as low as $\rho = 975$ and as high as $\rho = 1575$. Since we wanted to guarantee that an outbreak will start and sustain in any of the regions, the value of $\rho = 1575$ was chosen. Cells highlighted in orange indicate that the simulation was stopped by reaching the maximum value of days.

Appendix E (Continued)

Table E1: Calibration Values

Region	Seed	1100	1175	1250	1325	1375	1575	Stable level	Quadrant	Population
1	22	0.67	0.73	0.77	0.80			1100	1	825,882
1	23	0.67	0.74	0.78	0.80			1100	1	825,883
1	20	0.64	0.74	0.77	0.80			1100	1	825,881
2	20	0.81	0.85	0.87	0.89			1100	1	551,896
3	22	0.26	0.81	0.85	0.87			1175	2	1,043,295
3	23	0.00	0.81	0.85	0.87			1175	2	1,043,296
3	20	0.03	0.21	0.85	0.87			1175	2	1,043,294
4	20	0.12	0.81	0.85	0.87			1175	3	781,549
5	20	0.01	0.33	0.85	0.88			1175	2	883,261
6	20	0.00	0.46	0.86	0.88			1175	2	680,586
7	22	0.00	0.00	0.84	0.87			1250	2	622,440
7	23	0.00	0.01	0.84	0.87			1250	2	622,441
7	20	0.00	0.03	0.75	0.88			1250	2	622,439
8	20	0.00	0.80		0.88			1175	1	1,025,364
9	22	0.00	0.01	0.85	0.88			1250	1	1,184,981
9	23	0.00	0.18	0.85	0.88			1250	1	1,184,982
9	20	0.00	0.02	0.56	0.88			1250	1	1,184,980
10	20	0.00	0.82	0.85	0.87			1175	3	654,410
11	20	0.01	0.81	0.86	0.88			1175	1	303,827
12	20	0.77	0.81	0.85	0.87			1100	2	520,710
13	22	0.75	0.81	0.85	0.87			1100	2	877,007
13	23	0.00	0.82	0.85	0.87			1175	2	877,007
13	20	0.63	0.82	0.85	0.87			1100	2	877,007
14	20	0.77	0.82	0.85	0.87			1100	2	482,113
15	22	0.79	0.82	0.85	0.87			1100	2	583,923
15	23	0.78	0.83	0.85	0.87			1100	2	583,924
15	20	0.20	0.82	0.85	0.87			1175	2	583,922
16	22	0.00	0.00	0.86	0.89			1250	1	503,078
16	23	0.00	0.37	0.87	0.89			1250	1	503,078
16	20	0.00	0.17	0.86	0.89			1250	1	503,078
17	20	0.00	0.00	0.00	0.85			1325	1	206,541
18	20	0.00	0.00	0.00	0.82			1325	3	527,595
19	20	0.00	0.07	0.83	0.86			1250	2	589,529
20	22	0.00	0.78	0.83	0.86			1175	3	661,273
20	23	0.00	0.78	0.82	0.86			1175	3	661,274
20	20	0.00	0.53	0.83	0.86			1175	3	661,272
21	22	0.00	0.00	0.05	0.75			1325	3	636,551
21	23	0.00	0.00	0.00	0.79			1325	3	636,551
21	20	0.00	0.01	0.09	0.79			1325	3	636,551
22	20	0.01	0.09	0.81	0.85			1250	3	423,964
23	22	0.00	0.55	0.85	0.88			1250	2	526,887
23	23	0.00	0.00	0.85	0.00			1250	2	526,887
23	20	0.00	0.20	0.85	0.88			1250	2	526,887
24	20	0.00	0.00	0.00	0.01	0.89	0.92	1375	2	349,645

Appendix E (Continued)

Table E1 (Continued)

Region	Seed	1100	1175	1250	1325	1375	1575	Stable level	Quadrant	Population
25	22	0.00	0.80	0.85	0.88			1175	2	557,295
25	23	0.00	0.00	0.85	0.88			1250	2	557,296
25	20	0.00	0.02	0.00	0.88			1325	2	557,294
26	22	0.75	0.81	0.85	0.87			1100	3	558,570
26	23	0.76	0.82	0.85	0.88			1100	3	558,571
26	20	0.00	0.82	0.85	0.87			1175	3	558,569
27	20	0.00		0.76	0.86			1250	3	600,291
28	20	0.00	0.01	0.00	0.84			1325	2	432,274
29	20	0.00	0.00	0.00	0.84			1325	3	679,908
30	22	0.00	0.00	0.02	0.85			1325	3	704,542
30	23	0.00	0.00	0.02	0.85			1325	3	704,542
30	20	0.00	0.00	0.11	0.85			1325	3	704,542
31	23				0.83	0.89		1325	2	469,209
31	22				0.01	0.89		1375	2	469,209
31	20				0.86	0.89		1325	2	469,209
32	22	0.00	0.80	0.84	0.88			1175	3	620,821
32	23	0.03	0.80	0.85	0.88			1175	3	620,821
32	20	0.05	0.80	0.85	0.88			1175	3	620,821
33	20	0.01	0.15	0.85	0.88			1250	3	738,985
34	22	0.00	0.79	0.84	0.87			1175	3	796,336
34	23	0.00	0.80	0.85	0.87			1175	3	796,337
34	20	0.01	0.67	0.85	0.87			1175	3	796,335
35	20	0.18	0.86	0.88	0.90			1175	1	819,897
35	22	0.00	0.86	0.88	0.90			1175	1	819,897
35	23	0.18	0.86	0.88	0.90			1175	1	819,897
36	20	0.00	0.84	0.88	0.89			1175	2	646,287
37	20	0.81	0.85	0.87	0.89			1100	3	959,906
38	22	0.77	0.82	0.85	0.88			1100	4	728,855
38	23	0.78	0.82		0.88			1100	4	728,856
38	20	0.77	0.82	0.85	0.88			1100	4	728,854
39	20	0.78	0.83	0.86	0.89			1100	3	574,441
40	20	0.00	0.00	0.01	0.13	0.90		1375	1	237,688
41	20	0.01	0.08	0.85	0.88			1250	3	630,763
42	22	0.00	0.81	0.85	0.87			1175	3	734,609
42	23	0.77	0.82	0.85	0.87			1100	3	734,610
42	20	0.09	0.82	0.85	0.87			1175	3	734,608
43	20	0.00	0.85	0.87	0.89			1175	2	553,986
44	20	0.00	0.16	0.88	0.90			1250	1	676,386
45	22	0.03	0.01	0.88	0.89			1250	2	432,107
45	23	0.06	0.84	0.88	0.89			1175	2	432,108
45	20	0.00	0.36	0.88	0.90			1250	2	432,106
46	20	0.01	0.85	0.88	0.90			1175	1	504,321
47	20	0.57	0.85	0.88	0.89			1100	1	524,514
48	20	0.81	0.84	0.87	0.89			1100	3	1,486,068

Appendix E (Continued)

Table E1 (Continued)

Region	Seed	1100	1175	1250	1325	1375	1575	Stable level	Quadrant	Population
49	20	0.00	0.00	0.88	0.90			1250	2	805,462
50	20	0.81	0.84	0.87	0.89			1100	2	500,730
51	20		0.00	0.89	0.90			1250	1	1,037,783
51	22	0.82	0.86	0.88	0.90			1100	1	1,037,784
51	23	0.82	0.86	0.89	0.90			1100	1	1,037,785
52	20	0.82	0.86	0.88	0.90			1100	2	424,182
53	20	0.83	0.87	0.88	0.90			1100	1	398,818
54	20	0.45	0.87	0.88	0.90			1175	1	613,411
55	20	0.80						975	1	456,488
55	23							975	1	456,488
55	25	0.80						975	1	456,488
55	22	0.80						1025	1	456,488
56	20	0.81	0.85	0.87	0.88			1100	2	352,193
57	20	0.81	0.86	0.88	0.90			1100	2	477,403
58	22	0.00	0.00	0.00	0.83	0.87	0.91	1325	3	476,761
58	23	0.00	0.00	0.01	0.82	0.87	0.91	1325	3	476,761
58	20	0.00	0.00	0.00	0.00	0.86	0.91	1375	3	476,761
59	20	0.58		0.82	0.85			1100	3	1,133,826
60	22	0.00	0.00	0.00	0.00	0.83	0.91	1375	4	249,559
60	23	0.00	0.00	0.00	0.00	0.46	0.91	1500	4	249,559
60	20	0.00	0.00	0.00	0.00	0.08	0.91	1425	4	249,559
61	20	0.00	0.00	0.00	0.85	0.87	0.91	1325	3	691,965
62	22	0.00	0.00	0.00	0.03	0.82	0.91	1375	4	299,429
62	23	0.00		0.00	0.10	0.83	0.91	1375	4	299,430
62	20	0.00	0.00	0.00	0.00	0.67	0.91	1375	4	299,428
63	20	0.00	0.00	0.00	0.01	0.87	0.91	1375	3	382,039
64	22	0.00	0.00	0.00	0.00	0.01	0.82	1575	4	418,971
64	23	0.00	0.00	0.00	0.00	0.00	0.83	1575	4	418,971
64	20	0.00	0.00	0.00	0.00	0.00	0.82	1575	4	418,971
65	22	0.00	0.00	0.17	0.83			1325	4	560,332
65	23	0.00	0.00	0.15	0.84			1325	4	560,333
65	20	0.00	0.00	0.00	0.57	0.86	0.91	1325	4	560,331
66	20	0.77	0.82	0.85	0.87			1100	2	678,365
67	20		0.80		0.88			1175	1	279,019
68	20	0.77	0.82	0.85				1100	1	759,546
69	20	0.76	0.81	0.84	0.86			1100	1	698,204
70	20	0.74	0.79	0.81	0.84			1100	1	160,339
70	22	0.75	0.79	0.81	0.84			1100	1	160,339
70	23	0.74	0.79	0.82	0.84			1100	1	160,339
71	20	0.00	0.85	0.88	0.90			1175	1	931,317
72	20	0.80	0.85	0.87	0.89			1100	2	550,109
73	20	0.79	0.84	0.87	0.88			1100	2	916,206
74	20	0.80	0.84	0.87	0.89			1100	2	348,460
74	22	0.80	0.84	0.87	0.89			1100	2	348,461

Appendix E (Continued)

Table E1 (Continued)

Region	Seed	1100	1175	1250	1325	1375	1575	Stable level	Quadrant	Population
74	23	0.80	0.84	0.87	0.89			1100	2	348,462
75	20	0.78	0.83	0.86	0.88			1100	2	214,324
76	22	0.81	0.84	0.87	0.88			1100	2	179,115
76	23	0.80	0.84	0.87	0.88			1100	2	179,115
76	20	0.00	0.84	0.86	0.88			1175	2	179,115
77	20	0.79			0.87			1100	2	684,373
77	22	0.79						1025	2	684,373
77	25	0.78						1100	2	684,373
78	20	0.80	0.83	0.86	0.88			1100	1	163,367
79									4	19,308,938
80	20	0.00	0.00	0.54	0.86			1250	1	1,472,902
81	22	0.23	0.79		0.85			1175	4	747,536
81	23		0.80					1175	4	747,536
81	20	0.08	0.80		0.85			1175	4	747,536
82	20	0.01	0.80	0.84	0.87			1175	1	213,118
82	22	0.22	0.80	0.84	0.87			1175	1	213,119
82	23	0.34	0.00	0.84	0.87			1250	1	213,120
83	20	0.09	0.80	0.84	0.86			1175	1	490,663
84	20	0.74	0.80	0.83	0.86			1100	1	282,906
85	20	0.00	0.68	0.84	0.87			1175	1	1,590,998
86	20	0.77	0.82	0.86	0.88			1100	1	589,289
86	22	0.77	0.82	0.86	0.88			1100	1	589,290
86	23	0.76	0.83	0.86	0.88			1100	1	589,291
87	20	0.77	0.82	0.85	0.87			1100	2	195,554
88	22	0.00		0.00	0.88			1325	3	1,156,204
88	23	0.00	0.06	0.85	0.88			1250	3	1,156,205
88	20	0.00	0.06	0.85	0.88			1250	3	1,156,203
89	22	0.00	0.81	0.86	0.87			1175	4	761,727
89	25	0.00	0.81	0.85	0.87			1175	4	761,727
89	20	0.00	0.00	0.85	0.87			1250	4	761,727
90	20	0.65	0.83	0.86	0.88			1100	1	910,743
91	20	0.00	0.81	0.86	0.89			1175	1	111,663
91	23	0.17	0.70	0.86	0.89			1175	1	111,663
91	22	0.00	0.09	0.86	0.89			1250	1	111,663
92	20	0.00	0.82	0.86	0.89			1175	2	408,805
93	22	0.01	0.05	0.86	0.89	0.90	0.93	1250	4	563,086
93	23	0.00	0.02	0.80	0.00	0.90	0.93	1250	4	563,086
93	20	0.00	0.60	0.86	0.89	0.90	0.93	1175	4	563,086
94	20	0.78	0.83	0.86	0.89			1100	1	261,837
94	22	0.78	0.83	0.86	0.88			1100	1	261,838
94	23	0.78	0.83	0.86	0.88			1100	1	261,839
95	22	0.77	0.81	0.85	0.87			1100	4	220,559
95	23	0.77	0.82	0.85				1100	4	220,560
95	20	0.77	0.81	0.85	0.87			1100	4	220,558

Appendix E (Continued)

Table E1 (Continued)

Region	Seed	1100	1175	1250	1325	1375	1575	Stable level	Quadrant	Population
96	22	0.75	0.80					1100	3	1,600,954
96	23	0.76	0.80					1100	3	1,600,954
96	20	0.46	0.80					1175	3	1,600,954
97	20	0.00	0.84	0.87	0.89			1175	1	775,896
98	20	0.79	0.83	0.86	0.88			1100	2	660,334
98	22	0.79	0.83	0.86	0.88			1100	2	660,335
98	23	0.79	0.83	0.86	0.88			1100	2	660,336
99	20	0.79	0.83	0.87				1100	2	391,654
100	20	0.00	0.11	0.85				1250	1	530,640
101	20	0.84	0.87	0.88	0.90			1100	1	391,281
102	20	0.25	0.87	0.89	0.90			1175	2	312,102
102	22	0.69	0.87	0.89	0.90			1100	2	312,102
102	23	0.69	0.87	0.89	0.90			1100	2	312,102
103	20	0.84	0.87	0.89	0.90			1100	1	648,020
104	20	0.81	0.84	0.86	0.88			1100	2	251,638
105	20	0.07	0.88	0.90	0.91			1175	1	774,876
106	20	0.83						1025	1	718,103
106	22	0.83						1025	1	718,103
106	25	0.83						1025	1	718,103
107	20	0.80	0.84	0.87	0.88			1100	1	638,594
108	20	0.00	0.85	0.88	0.90			1175	1	799,418
109	20	0.00	0.84	0.88	0.89			1175	1	486,713
109	22	0.00	0.85	0.87	0.89			1175	1	486,714
109	23	0.00	0.85	0.87	0.89			1175	1	486,715
110	20	0.22	0.84					1175	2	698,654
110	22	0.23	0.84					1175	2	698,654
110	25	0.00	0.85					1200	2	698,654
111	20	0.02	0.85	0.88	0.89			1175	2	592,141
112	20	0.80	0.84	0.87	0.89			1100	3	1,279,590
113	20	0.80	0.84	0.86	0.88			1100	3	416,539
114	20	0.07	0.83	0.87	0.89			1175	1	563,483
115	20	0.00	0.00	0.86	0.88			1250	3	435,114
116	20	0.00	0.84	0.87	0.88			1175	3	528,557
116	22	0.79	0.84	0.87	0.88			1100	3	528,558
116	23	0.80	0.84	0.87	0.88			1100	3	528,559
117	20	0.00	0.00	0.01	0.84			1325	1	423,728
118	20	0.00	0.78	0.84	0.86			1175	3	225,008
119	20	0.75	0.80	0.84	0.86			1100	2	119,061
120	20	0.00	0.00	0.15	0.82			1325	3	436,736
121	22	0.00			0.54	0.856		1325	3	1,314,400
121	23				0.72	0.86		1325	3	1,314,400
121	20	0.00			0.00	0.809		1400	3	1,314,400
122	20	0.00	0.10	0.82	0.86			1250	3	759,493
123	20	0.00	0.01	0.87	0.90			1250	1	446,808

Appendix E (Continued)

Table E1 (Continued)

Region	Seed	1100	1175	1250	1325	1375	1575	Stable level	Quadrant	Population
123	22	0.00	0.00	0.61	0.90			1250	1	446,808
123	23	0.00	0.00	0.88	0.90			1250	1	446,808
124	20	0.69	0.88	0.89	0.91			1100	1	613,709
125	20	0.01	0.85	0.89	0.91			1175	1	212,892
126	20	0.85	0.88	0.89	0.90			1100	1	492,055
127	20	0.85	0.87	0.89	0.90			1100	1	519,985
128	20	0.85	0.87	0.89	0.90			1100	1	635,905
129	20	0.84	0.86	0.88				1100	2	568,792
130	20	0.61	0.87	0.89	0.91			1175	1	195,868
131	20	0.83	0.87	0.89	0.90			1100	1	311,157
132	20	0.82	0.85	0.87	0.88			1100	1	333,800
133	20	0.84	0.86	0.87	0.89			1100	1	184,008
134	20	0.70	0.77	0.81	0.84			1100	2	237,878
135	20	0.72	0.79	0.83	0.85			1100	1	263,524
136	20	0.01	0.78	0.83	0.86			1175	1	70,684
137	23	0.00			0.56	0.83	0.89	1325	4	212,788
137	22	0.00		0.00	0.00	0.83	0.89	1425	4	212,788
137	20	0.00		0.01	0.01	0.84	0.89	1425	4	212,788
138	22	0.00	0.00	0.01	0.00	0.01	0.90	1575	4	56,359
138	23	0.01	0.00	0.01	0.00	0.00	0.90	1575	4	56,360
138	20	0.01	0.02	0.00	0.79			1325	4	56,358
139	22	0.00	0.00	0.14	0.61	0.87	0.91	1325	4	90,242
139	23	0.00	0.00	0.01	0.01	0.87	0.91	1375	4	90,242
139	20	0.00	0.00	0.06	0.84	0.84	0.91	1325	4	90,242
140	20	0.00	0.46	0.82	0.85			1250	3	1,155,364
141	20	0.00	0.00	0.00	0.85			1325	1	246,271
142	20	0.00		0.11	0.83		0.90	1325	3	292,553
142	22	0.00		0.00	0.83		0.90	1325	3	292,553
142	23	0.00		0.05	0.84		0.90	1325	3	292,553
143	20	0.00	0.00	0.81	0.86			1250	3	727,500
144	23	0.00	0.02	0.81	0.85			1250	4	303,368
144	22	0.00	0.01	0.33	0.85			1325	4	303,368
144	20	0.00	0.00	0.78	0.86			1250	4	303,368
145	22	0.74	0.81	0.85	0.87			1100	4	378,870
145	23	0.75	0.81	0.85	0.87			1100	4	378,871
145	20	0.00	0.81	0.85	0.87			1175	4	378,869
146	20		0.00	0.01	0.89			1325	1	58,972
147	20	0.77	0.82	0.85	0.87			1100	2	326,394
148	20	0.61	0.78	0.81	0.85			1100	2	133,106
149	20	0.03	0.78	0.83	0.86			1175	3	387,716
150	20	0.00	0.00	0.00	0.00	0.57	0.63	1375	3	1,485,310
151	20	0.00	0.00	0.00	0.84			1325	3	510,367
151	22	0.00	0.05	0.80	0.84			1250	3	510,368
151	23	0.00	0.00	0.00	0.84			1325	3	510,369

Appendix E (Continued)

Table E1 (Continued)

Region	Seed	1100	1175	1250	1325	1375	1575	Stable level	Quadrant	Population
152	20	0.00	0.00	0.00	0.78			1325	3	860,288
153	20	0.23	0.80	0.84	0.87			1175	3	877,498
154	20	0.00	0.00	0.55	0.87			1325	1	136,762
155	20	0.31	0.81	0.84	0.87			1175	1	58,180

Appendix F

List of Economically Undeveloped Regions

Table F1: List of Economically Undeveloped Regions

Region	Population
5. Tierra Blanca, Veracruz	883,261
6. Martínez de la Torre, Veracruz	680,586
7. Tantoyuca, Veracruz	622,439
8. Poza Rica de Hidalgo, Veracruz	1'025,364
9. Coatepec, Veracruz	1'184,980
10. Veracruz, Veracruz	654,410
11. San Andrés Tuxtla, Veracruz	303,827
12. Córdoba, Veracruz	520,710
13. Coatzacoalcos, Veracruz	877,007
14. Xalapa, Veracruz	482,113
15. Tlaxcala de Xicohténcatl, Tlaxcala	583,922
16. Huamantla, Tlaxcala	503,078
23. Macuspana, Tabasco	526,887
24. Cunduacán, Tabasco	349,645
25. Cárdenas, Tabasco	557,294
26. Villahermosa, Tabasco	558,569
43. Tehuacan, Puebla	553,986
44. Huauchinango, Puebla	676,386
45. Teziutlan, Puebla	432,106
46. Atlixco, Puebla	504,321
47. Amozoc de Mota, Puebla	524,514
48. Puebla de Zaragoza, Puebla	1'486,068
49. Palmar de Bravo, Puebla	805,462
50. San Martin Texmelucan de Labastida, Puebla	500,730
51. Santiago Pinotepa Nacional, Oaxaca	1'037,783
52. San Juan Bautista Valle Nacional, Oaxaca	424,182
53. Huajuapan de León, Oaxaca	398,818
54. Santo Domingo Tehuantepec, Oaxaca	613,411
55. Oaxaca de Juárez, Oaxaca	456,488
56. Salina Cruz, Oaxaca	352,193
57. San Juan Bautista Tuxtepec, Oaxaca	477,403
68. Yautepec de Zaragoza, Morelos	759,546
69. Cuernavaca, Morelos	698,204
70. Cuautla, Morelos	160,339

Appendix F (Continued)

Table F1 (Continued)

Region	Population
71. Puruándiro, Michoacán	931,317
72. Zitácuaro, Michoacán	550,109
73. Uruapan, Michoacán	916,206
74. La Piedad de Cabadas, Michoacán	348,460
75. Pátzcuaro, Michoacán	214,324
76. Apatzingán de la Constitución, Michoacán	179,115
77. Morelia, Michoacán	684,373
78. Ciudad Lázaro Cárdenas, Michoacán	163,367
80. Ixtlahuaca de Rayón, México	1'472,902
81. Toluca de Lerdo, México	747,536
82. Amecameca de Juárez, México	213,118
83. Texcoco de Mora, México	490,663
84. Metepec, México	282,906
85. Tenancingo de Degollado, México	1'590,998
97. Tula de Allende, Hidalgo	775,896
98. Pachuca de Soto, Hidalgo	660,334
99. Tulancingo, Hidalgo	391,654
100. Huejutla de Reyes, Hidalgo	530,640
101. Chilpancingo de los Bravo, Guerrero	391,281
102. Teloloapan, Guerrero	312,102
103. Ixtapa Zihuatanejo, Guerrero	648,020
104. Iguala de la Independencia, Guerrero	251,638
105. Tlapa de Comonfort, Guerrero	774,876
106. Acapulco de Jurez, Guerrero	718,103
123. Tila, Chiapas	446,808
124. Ocosingo, Chiapas	613,709
125. Chiapa de Corzo, Chiapas	212,892
126. Venustiano Carranza, Chiapas	492,055
127. Villaflores, Chiapas	519,985
128. Tapachula, Chiapas	635,905
129. Tuxtla Gutiérrez, Chiapas	568,792
130. La Trinitaria, Chiapas	195,868
131. Reforma, Chiapas	311,157
132. San Cristóbal de las Casas, Chiapas	333,800
133. Comitán de Domínguez, Chiapas	184,008

Appendix G

List of Likely Pandemic Export Regions

Table G1: List of Likely Pandemic Export Regions

Region	Population	Category
18. Matamoros, Tamaulipas	527,595	Border
21. Reynosa, Tamaulipas	636,551	Border
22. Nuevo Laredo, Tamaulipas	423,964	Border
29. Nogales, Sonora	679,908	Border
39. Cancún, Quintana Roo	574,441	Tourist
65. Linares, Nuevo Len	560,331	Border
79. Ciudad de México, D.F.	19'308,938	Major city
95. Puerto Vallarta, Jalisco	220,558	Tourist
96. Guadalajara, Jalisco	1'600,954	Major City
117. Guadalupe y Calvo, Chihuahua	423,728	Border
120. Cuauhtémoc, Chihuahua	436,736	Border
121. Ciudad Juárez, Chihuahua	1'314,400	Border
137. Ciudad Acuña, Coahuila	212,788	Border
138. San Buenaventura, Coahuila	56,358	Border
142. Piedras Negras, Coahuila	292,553	Border
149. La Paz, Baja California Sur	387,716	Tourist
150. Tijuana, Baja California	1'485,310	Border
151. Ensenada, Baja California	510,367	Border
152. Mexicali, Baja California	860,288	Border

Appendix H

Results on the Normality of the Regression Model

The following figure shows that the errors followed a normal distribution. Consequently, parametric statistics was used to analyze the results of the models.

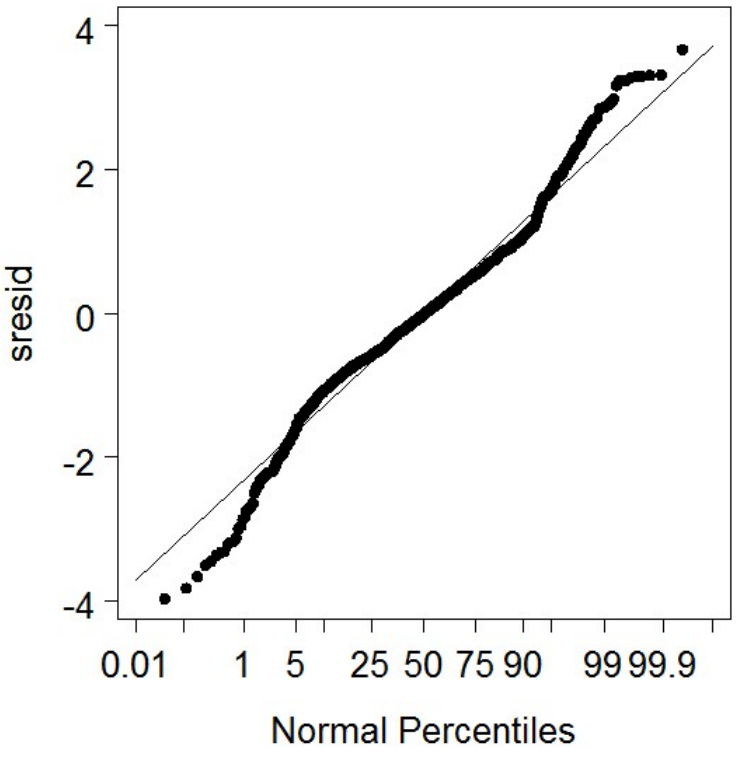

Figure H1: Results on the Normality of the Regression Model

Appendix I

Histogram of Lead Time

The following figure shows a histogram of the lead time not considering the cases when the outbreak was contained at the source.

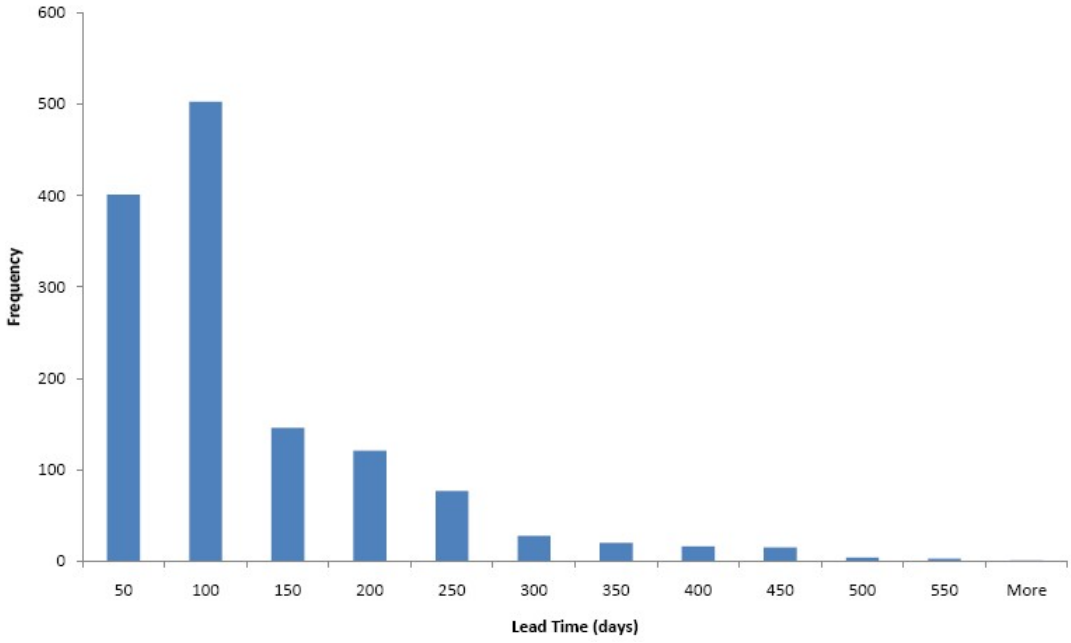

Figure I1: Histogram of Lead Time

Appendix J

Percentage of Containment at the Source

The following table shows the percentage of the time that an outbreak was contained at the source given certain strategy.

Table J1: Percentage of Containment at the Source

AD	AS	NPI	D	% Containment
2	2,000,000	1	24	98%
3	260,000	1	24	98%
3	2,000,000	1	24	98%
3	2,000,000	1	240	98%
2	2,000,000	1	240	98%
3	2,000,000	0	24	98%
3	260,000	1	240	96%
3	260,000	1	720	93%
3	2,000,000	1	720	93%
2	2,000,000	1	720	91%
2	2,000,000	0	24	87%
3	2,000,000	0	240	87%
2	260,000	1	24	85%
2	260,000	1	240	81%
2	260,000	1	720	70%
2	2,000,000	0	240	69%
2	260,000	0	24	26%
1	260,000	1	720	23%
1	2,000,000	1	24	23%
1	2,000,000	1	720	23%
1	260,000	1	24	22%
1	260,000	1	240	22%
1	2,000,000	1	240	22%
3	260,000	0	24	21%
2	260,000	0	240	17%
3	260,000	0	240	15%
1	-	1	240	9%
3	2,000,000	0	720	7%
1	-	1	24	6%
2	2,000,000	0	720	6%
1	-	1	720	6%
1	-	0	24	0%
1	-	0	240	0%
1	-	0	720	0%
1	260,000	0	24	0%
1	260,000	0	240	0%
1	260,000	0	720	0%
1	2,000,000	0	24	0%
1	2,000,000	0	240	0%
1	2,000,000	0	720	0%
2	260,000	0	720	0%
3	260,000	0	720	0%

About the Author

Alfredo Santana Reynoso earned his B.S. in Industrial Engineering with a minor in Systems Engineering from Monterrey Institute of Technology, Mexico in 1999. He received his M.E. in Project Engineering from the University of Guadalajara, Mexico. He is expected to obtain his Ph.D. in Industrial Engineering from the University of South Florida in August of 2011. He began his academic career at Panamericana University, Mexico in 2004. Since then he has been the instructor of several undergraduate courses, including: Introduction to Industrial Engineering, Project Management, Facilities Design and Planning, and Inventory Management (all taught in Mexico), and Production Control, Project Management, and Deterministic Operations Research at the University of South Florida. He also worked in the glass manufacturing and food industries as a Software Designer, Production Planner and Manager, Technical Manager, and Corporative Project Manager. His research interest include analysis and modeling of complex systems, computer simulation, geographic optimization, analytics, business intelligence, and decision and risk analysis.